Doctoral Thesis

Graz University of Technology

Finite Element Techniques for Three-Dimensional Skin Effect Problems

Imam Bakhsh

Institute for Fundamentals and Theory in Electrical Engineering
Graz University of Technology, Austria

Supervisor and 1^{st} Reviewer:
Univ.-Prof. Dipl.-Ing. Dr. techn. Oszkár Bíró
Graz University of Technology, Austria

2^{nd} Reviewer:
Univ.-Doz. Dr. Bernhard Brandstätter
Leiter Forschung und Entwicklung
ELIN Motoren GmbH, Austria

Graz, March 2012

Kurzfassung

In der Konstruktion und Analyse von elektromagnetischen Geräten ist die Bestimmung der Stromdichte sowie des Magnetfeldes in verschiedenen Konstruktionsteilen äußerst wichtig. Speziell für Probleme mit komplexer Geometrie ist eine dreidimensionale (3D) Analyse im Frequenz- oder Zeitbereich notwendig. Die Methode der finiten Elemente (FEM) wird sehr häufig für solche Analysen verwendet. In dieser Arbeit werden zwei mögliche Formulierungen für 3D - Stromverdrängungsprobleme untersucht. Die sogenannte $(\mathbf{A}, v - \mathbf{A})$ Formulierung verwendet das magnetische Vektorpotential $\mathbf{A}$ im gesamten Problembereich zusätzlich zu dem in leitfähigen Gebieten verwendeten zeitintegrierten elektrischen Skalarpotential v.

In der $(\mathbf{T}, \Phi - \Phi)$ Formulierung werden die Feldgrößen einerseits mit dem Strömungsvektorpotential $\mathbf{T}$, welches in nichtleitenden Gebieten bekannt und sonst unbekannt ist und andererseits zusätzlich mit dem magnetischen Skalarpotential Φ im gesamten Problemgebiet beschrieben. Die Vektorpotentiale werden bei der FEM vorteilhaft durch Kantenbasisfunktionen (Kantenelemente) und die skalaren Potentiale durch Knotenbasisfunktionen (Knotenelemente) angenähert.

Stromverdrängungsprobleme sind eine spezielle Klasse von Wirbelstromproblemen mit der Vorschreibung von Spannung oder Strom. Auf die Komplementarität der beiden Formulierungen wird hingewiesen. Es wird gezeigt, dass die Spannungsvorgabe eine starke globale Zwangsbedingung bei der $(\mathbf{A}, v - \mathbf{A})$ Formulierung und ein natürlicher Weg zur Kopplung mit den Potentialfunktionen ist, während bei der $(\mathbf{T}, \Phi - \Phi)$ Formulierung die Spannungsvorgabe eine schwache Bedingung ist, die zur Realisierung die Einführung eines speziellen eingeprägten Vektorpotentials erfordert. Auf der anderen Seite ist die Stromvorgabe eine starke globale Bedingung für die $(\mathbf{T}, \Phi - \Phi)$ Formulierung und stellt einen natürlichen Weg zur Kopplung mit den Potentialfunktionen dar, während die Strombedingung im Fall der $(\mathbf{A}, v - \mathbf{A})$ Formulierung eine schwache globale Bedingung ist, die zur Realisierung der Einführung eines speziellen Skalarpotentials bedarf.

Die Beschreibung der Implementierung der Stromvorgabe bei der $(\mathbf{A}, v - \mathbf{A})$ Formulierung ist neu in der vorliegenden Arbeit. Des Weiteren neu ist Erweiterung der vorstellten Methode auf transiente Wirbelstromprobleme. Die Validierung der beschriebenen Verfahren wird durch Vergleich mit mittels herkömmlicher Methoden gelöster Beispiele durchgeführt, wobei eine ausgezeichnete Übereinstimmung erzielt wird. Im letzten Schritt wird die neue Methode auf einige industrielle Probleme angewendet.

Abstract

Determining the current density distribution as well as the magnetic flux distribution in different parts is extremely important in the design and analysis of electromagnetic appliances. Three dimensional analysis, in frequency or time domain, especially for problems with complex geometries is required. The finite element method (FEM) is widely used for such kind of analyses. In this work, two potential formulations are studied for 3D skin effect problems. The $\mathbf{A}, v - \mathbf{A}$ formulation uses the magnetic vector potential in the entire problem domain and additionally, the time integrated electric scalar potential in the eddy current region. In the $\mathbf{T}, \Phi - \Phi$ formulation, the field quantities are expressed with the current vector potential $\mathbf{T}$ known in the domain free of eddy currents and unknown elsewhere. The magnetic scalar potential Φ is used in the whole problem domain. In a finite element context, the vector potentials are advantageously approximated by edge basis functions whereas the scalar potentials are expanded by node based ones.
The skin effect problem is a special class of eddy current problem with the prescription of either the voltage or the current. Compelementarity of the two formulations is pointed out. It is shown that the voltage prescription condition is a strong global constraint for the $\mathbf{A}, v - \mathbf{A}$ formulation and a natural way of coupling with the potential functions whereas in case of the $\mathbf{T}, \Phi - \Phi$ formulation, this condition is a weak global constraint and needs a magnetic source potential function to be introduced. On the other hand, the current prescription condition is a strong global constraint for the $\mathbf{T}, \Phi - \Phi$ formulation and a natural way of coupling with potential functions whereas in case of the $\mathbf{A}, v - \mathbf{A}$ formulation, this condition is a weak global constraint and needs the source electric scalar potential corresponding to the source of a unit potential, in terms of the scalar basis function obtained as the sum of the nodal basis functions corresponding to the nodes on the electrodes with given current condition. The treatment and implementation of the current condition in the $\mathbf{A}, v - \mathbf{A}$ formulation is a new feature in this work. The newly developed technique is extended to transient skin effect problems in the time domain too. The validation of the technique was carried out by selecting and solving problems which could be tackled by existing techniques as well. Excellent agreement was obtained during the comparison of the results. In the next step, it was applied to some industrial problems.

Acknowledgement

First of all, I am grateful to Almighty Allah, the beneficent, the merciful and the lord of the Universe, for all the blessings He has incessantly showered upon me. And I offer the best of salutations to all his messengers especially to his last and noble prophet Muhammad, peace and blessings be upon him.
Special thanks go to my supervisor, Professor Oszkár Bíró, for leading me to the area of Computational Mathematics in Electrical Engineering with his excellent guidance, support and encouragement.
Furthermore, I would like to thank Dr. Andrej Stermecki, who cooperated with me in the project and provided me help working with ANSYS.
I would also like to thank Dr. Bernhard Brandstätter for being the second reviewer for this thesis.
Many thanks to my family for their continuous support and to all my friends and relatives in Pakistan, Austria and all over the world.
The research work for this doctoral thesis was carried out with the funding provided by Higher Education Commission (HEC) Pakistan. I am thankful to the people of Pakistan who are the real financial supporter of this work indirectly.
Finally, I would like to thank everybody in IGTE for the wonderful time we had during my Ph.D. studies.

Graz, March 2012 Imam Bakhsh

Contents

List of Figures

List of Tables

Chapter 1

Introduction

The skin effect problem is the magneto-dynamic problem of finding the current density distribution in an arbitrary system of current carrying conductors. Displacement effects are considered negligible [3, 4]. The skin effect problems are in fact a special class of eddy current fields described by means of partial differential equations coupled to the external source voltages or currents. These equations are formulated in terms of potential functions from which field quantities are easily retrievable. A lot of work has already been done in developing various potential formulations describing eddy current fields both in two and three dimensions [5,6]. Mixed potential formulations, using both vector and scalar potentials, approximated either by means of nodal elements or by means of edge elements [5], are now available to get unique solutions [7] for the potential functions [8]. Either the magnetic vector potential, $\mathbf{A}$ and the electric scalar potential, V or the current vector potential (also named as electric vector potential in some literature), $\mathbf{T}$ and the magnetic scalar potential, Φ are used in conducting regions, whereas the magnetic field in nonconducting regions is described by $\mathbf{A}$ or Φ [9]. For nodal based approximations of the potential functions two excellent overviews on the differential formulations are given in [9] and [10]. Use of the edge elements for the approximation of potentials is summarized in [11] for different possible formulations.

1.1. Literature review

These problems have been investigated for a long time. Analytical techniques [12] applied initially resulted in useful results for conductors of simple shapes. The first attacking of such problems with arbitrary geometries was made by Silvester [13] in 1968, using numerical techniques [14, 15]. He used the modal theory of current flow to make an eigenvalue problem and using the network analysis subroutines to produce the skin effect curves in terms of AC and DC resistance and inductance ratios. Afterwards, the finite element method [16, 17] was applied to two dimensional skin effect problems by many other authors too including M. V. K. Chari [18], Z. J. Csendes, A. Konrad [19] and I. D. Mayergoyz [20].

In [20] a modification to the mathematical formulation of skin effect problems is proposed to make it possible to trace the skin effect in 3-D problems and perfect conductors. The idea was to introduce filamentary or virtual current carrying conductors in the actual conductor. The field equations outside the conducting region are so comprised that the total current in the conductors appear explicitly in the formulation through the boundary conditions. Boundary integral method is used for the realization of the formulation.

A scheme to model the skin depth in massive conductors is presented with voltage and current forced conditions in the finite element $A\Psi V$ formulation in [21]. Nodal based shape functions have been used with the enforcement of the coulomb gauge. First order iso-parametric brick and second order hierarchical elements have been used. It is shown that higher order elements can give better results for skin depth.

In [22] a finite element formulation for 3-D current driven problems is presented which uses potential functions to represent the field quantities. An impressed current vector potential is used to describe an arbitrary current distribution in the conductors corresponding to the net given current. Edge elements have been used for the representation of the impressed current vector potential and nodal elements for the magnetic scalar potential in the whole problem domain. Options for the selection of the impressed vector potential have been discussed thoroughly.

Study of two potential formulations, $\mathbf{T}, \Omega$ and $\mathbf{A}, \Psi$ coupled with electric circuit equations is presented in [23] and [24]. Here, hybrid elements are used with the enforcement of the gauge condition, by setting the vector potential component along the tree edges equal to zero.

In [25] the choice of nodal or edge finite elements for the expansion of magnetic vector potential and its gauging is explored, specially when higher order elements are used in the finite element analysis of 3-D magnetostatic problems. Recommendation for the edge elements for ungauged vector potential has been made for better numerical stability and accuracy. The solution of singular system of equations is obtained by iterative solvers like ICCG, provided the consistence of the right hand side is ensured.

In [26–30] coupling of magnetic vector potential formulation and H-formulations with global quantities is given and the use of source fields associated with both formulations in connection with voltage and current sources is proposed. The complementarity of the two formulations has also been elaborated.

A comparison of a few finite element formulations for two dimensional eddy current problems is presented in [31]. These formulations are based on a single component magnetic vector potential for current sources only. One of these formulations takes

into account the proximity and skin effects. A mesh adaptation procedure is given for such problems with integro-differential formulation, for example in [32]

1.2. Outline of the thesis

In the next Section of this *chapter*, a brief description of the Galerkin method is presented.

In *chapter 2*, the field model of the eddy current problem and the skin effect problem is presented. The differential equations and boundary conditions for both problems are shown in terms of the field quantities. The two potential formulations, the $\mathbf{A}, v - \mathbf{A}$ and the $\mathbf{T}, \Phi - \Phi$, for the eddy current problem are introduced.

In *chapter 3*, the skin effect problem with prescribed voltage condition is presented. The $\mathbf{A}, v - \mathbf{A}$ formulation naturally suites the voltage as a global constraint to be incorporated in terms of the modified electric scalar potential. The coupling of global quantities with potential formulations is presented.

In *chapter 4*, it is shown that the incorporation of the given current condition in the $\mathbf{T}, \Phi - \Phi$ formulation is natural with the use of the impressed current vector potential.

In contrast, in *chapter 5* it is presented that the $\mathbf{T}, \Phi - \Phi$ formulation needs additional treatment to incorporate the condition of voltage excitation. This is achieved by assuming filamentary currents for the voltage sources. The source field function is used to account for the unknown current of source or around the hole to establish the circuit relation in the Galerkin finite element equations.

The $\mathbf{A}, v - \mathbf{A}$ formulation, for skin effect problems with prescribed current condition, is presented in *chapter 6*. The Dirichlet boundary condition, in this formulation, is not completely specified. The treatment of the partially specified boundary condition, on the electrodes with given current condition, is shown and implemented in the software environment(EleFAnT 3D, developed at IGTE). In this case the introduction of a unit source electric scalar potential facilitates to establish the relation between the potentials and the given currents of the sources in the weak form.

The treatment of transient skin effect problems is shown in *chapter 7*. The time stepping technique is described for general nonperiodic excitations. It is shown that the time difference technique using linear interpolation gives the discretized system of equations. Stepping through several periods is necessary, with this approach, to obtain the steady state solution of time periodic skin effect problems approximately. It is also shown that transient problems with time periodic excitations can be solved both in

the frequency and the time domain at the cost of stepping through one period only. Nonlinearity of the transient problems is taken into account with the use of the fixed point method.

In *chapter 8*, for validation purposes, the results of the two potential formulations are compared for a thick conductor coil problem. Furthermore an industrial problem is solved with the newly developed technique i.e. the $\mathbf{A}, v-\mathbf{A}$ formulation generalized for the given current condition. Higher harmonic losses are computed in the short circuit ring of a 14 pole induction motor. Analysis is performed at the preselected harmonics, $300Hz$, $600Hz$ and $1200Hz$. The validation of the technique, the $\mathbf{A}, v-\mathbf{A}$ formulation with current sources, for transient skin effect problems is done by solving the thick conductor coil problem, already solved for the steady state case, with time stepping technique and discrete frequency domain analysis.

Finally, the conclusion of the work is given in *chapter 9*.

1.3. Galerkin's finite element technique

The first step in the numerical solution of the partial differential equations is to reduce them to a system of algebraic equations for static and stationary field problems, or to a system of ordinary differential equations for time dependent fields. This is done by using variational techniques in most of the cases [33]. The system of ordinary differential equations of the transient case simplifies to a complex algebraic equations system for time harmonic problems in which case the operator of the time derivation reduces to a simple multiplication by $j\omega$ ($\frac{\partial}{\partial t} \Rightarrow j\omega$), where ω is the angular frequency. To cover the general case of transient problems Galerkin's method is the most general and suitable one.

In the application of Galerkin's method, the Dirichlet boundary conditions are satisfied exactly while the Neumann boundary conditions are approximated [34]. This leads in the static case to the same solution which is obtained by applying the Ritz's method [35].

For transient eddy current field problems, the differential equation to be solved has the following form

$$L_2 u + L_t \frac{\partial u}{\partial t} = f \qquad \text{in } \Omega, \tag{1.1}$$

where u is the unknown function to be evaluated and f is the known forcing function. L_2 is a second order elliptic differential operator and L_t a symmetric operator with respect to any arbitrary function w and the function u such that

$$\int_\Omega (L_t u)\, w \; d\Omega = \int_\Omega u\, (L_t w) \; d\Omega. \tag{1.2}$$

The boundary and initial conditions to be satisfied are

$$L_D u = g \qquad \text{on } \Gamma_D, \tag{1.3}$$

$$L_N u = h \qquad \text{on } \Gamma_N, \tag{1.4}$$

$$u(t=0) = u_0, \tag{1.5}$$

where g and h are the known functions to be specified on the disjunct parts Γ_D and Γ_N of the boundary Γ, i. e. Dirichlet and Neumann boundary conditions are specified on the corresponding surfaces. The operator L_D is the identity operator if u is a scalar function or it yields the tangential or the normal component of u if the latter is a vector function. The operator L_N denotes some kind of partial derivation such as $n \times curl$ or $n \cdot grad$. The differential equation (1.1) and the Neumann boundary condition (1.4) can be combined to write the operator equation as

$$L_2 u + L_t \frac{\partial u}{\partial t} + \delta_{\Gamma_N} L_N u = f + \delta_{\Gamma_N} h \qquad \text{in } \Omega. \tag{1.6}$$

The function δ_{Γ_N} is a Dirac distribution concentrated on the surface Γ_N, i.e.

$$\delta_{\Gamma_N}(P) = \begin{cases} 0 & \text{if } P \notin \Gamma_N \\ \infty & \text{if } P \in \Gamma_N \end{cases} \tag{1.7}$$

which satisfies

$$\int_\Omega \delta_{\Gamma_N} w \, d\Omega = \int_{\Gamma_N} w \, d\Gamma, \tag{1.8}$$

with w any arbitrary function. To obtain the weak form of the boundary value problem, the operator equation (1.6) is multiplied by any weighting function w and integrated over the problem domain Ω

$$\int_\Omega \left(L_2 u + L_t \frac{\partial u}{\partial t} - f \right) w \, d\Omega + \int_{\Gamma_N} \left(L_N u - h \right) \left(L_D w \right) \, d\Gamma = 0 \qquad \forall w, \tag{1.9}$$

with $L_D w = 0$ on Γ_D. It can be seen from the above equation that, for any function w, the differential equation (1.1) and the Neumann boundary condition (1.3) are satisfied. Of course, the fundamental lemma of the variational calculus is assumed to be valid, i.e. if G is a continuous function and

$$\int_\Omega G w \, d\Omega = 0 \tag{1.10}$$

for w arbitrary with

$$w(\partial\Omega) = 0 \tag{1.11}$$

then

$$G = 0 \qquad \text{identically within } \Omega, \tag{1.12}$$

Application of the partial integration to the equation (1.9) will in general be a Green's identity of the form

$$\int_\Omega (L_2 u)\, w \; d\Omega = \int_\Omega (L_1 u)\,(L_1 w) \; d\Omega - \oint_\Gamma (L_N u)\, w \; d\Gamma = 0, \tag{1.13}$$

where L_1 is a first order differential operator. The unknown function u is approximated by means of an entire function set $\{f_k\}$

$$u^{(n)}(\mathbf{r}, t) = u_D(\mathbf{r}, t) + \sum_{k=1}^{n_1} u_k(t) f_k(\mathbf{r}). \tag{1.14}$$

The time dependence of the unknown coefficients u_k is shown explicitly for the general case of transient field problems. The symbol n_1 denotes the number of degrees of freedom of the approximate function $u^{(n)}$. The function u_D satisfies the inhomogenous (1.3) and the expansion functions f_k the homogenous Dirichlet boundary conditions

$$L_D f_k = 0 \qquad \text{on } \Gamma_D. \tag{1.15}$$

The initial solution u_0 in (1.5) can be approximated as

$$u_0^{(n)} = \sum_{k=1}^{n_1} u_{0k} f_k, \tag{1.16}$$

therefore initial values can be assigned to u_k

$$u_k(t = 0) = u_{0k}. \tag{1.17}$$

Choosing an entire function set $\{f_k\}$ of n_1 elements satisfying the homogenous Dirichlet boundary conditions (1.15), Galerkin's equations are obtained from (1.9) using Green's identity

$$\int_\Omega \left(L_1 u^{(n)}\right)(L_1 f_k) \; d\Omega + \frac{\partial}{\partial t} \int_\Omega \left(L_t u^{(n)}\right) f_k \; d\Omega = \int_\Omega f f_k \; d\Omega + \int_{\Gamma_N} h\,(L_D f_k) \; d\Gamma, \qquad k = 1, 2, \cdots, n_1. \tag{1.18}$$

Inserting (1.14) into (1.18), a system of ordinary differential equation can be written:

$$\mathbf{A}\mathbf{u} + \frac{\partial}{\partial t}(\mathbf{B}\mathbf{u}) = \mathbf{f}. \tag{1.19}$$

The elements of $\mathbf{u}$ are the coefficients u_k and the elements of matrices $\mathbf{A}$, $\mathbf{B}$ and vector $\mathbf{f}$ are:

$$A_{ik} = \int_\Omega (L_1 f_i)\,(L_1 f_k) \; d\Omega, \tag{1.20}$$

$$B_{ik} = \int_{\Omega} (L_t f_i)\, f_k \, d\Omega, \tag{1.21}$$

$$f_i = \int_{\Omega} f f_i \, d\Omega + \int_{\Gamma_N} h\,(L_D f_i) \; d\Gamma - \int_{\Omega} (L_1 u_D)\,(L_1 f_i) \; d\Omega. \tag{1.22}$$

There are normally two unknown potential functions introduced in most of the formulations of eddy current fields, specially the two formulations used in this work. If the boundary value problem consists of two governing differential equations with two unknown functions u and v, then the operators themselves are matrices ($\mathbf{L}_2$ and $\mathbf{L}_t$) and the Galerkin equations (1.19) change to:

$$\begin{bmatrix} \mathbf{A}_{uu} & \mathbf{A}_{uv} \\ \mathbf{A}_{vu} & \mathbf{A}_{vv} \end{bmatrix} \begin{Bmatrix} \mathbf{u} \\ \mathbf{v} \end{Bmatrix} + \begin{bmatrix} \mathbf{B}_{uu} & \mathbf{B}_{uv} \\ \mathbf{B}_{vu} & \mathbf{B}_{vv} \end{bmatrix} \left\{ \begin{Bmatrix} \dot{\mathbf{u}} \\ \dot{\mathbf{v}} \end{Bmatrix} \right\} = \begin{Bmatrix} \mathbf{f} \\ \mathbf{g} \end{Bmatrix} \tag{1.23}$$

with the function v approximated by n_2 elements of an entire function set $\{g_k\}$ as

$$v^{(n)}(\mathbf{r}, t) = v_D(\mathbf{r}, t) + \sum_{k=1}^{n_2} v_k(t) g_k(\mathbf{r}) \tag{1.24}$$

where n_2 stands for the degrees of freedom of the approximating function $v^{(n)}$ and the known vector $\mathbf{g}$ consists, similarly to $\mathbf{f}$, of integrals of the products of the forcing function and the expansion functions over the problem domain Ω. The symmetry of the matrices $\mathbf{A}$ and $\mathbf{B}$ is numerically advantageous.

An important step in the classical Galerkin method is the selection of trial functions defined over the entire solution domain that can represent the true solution, at least approximately. For most two and three dimensional problems it is very difficult to find such functions. To alleviate this difficulty, the entire domain is subdivided into small subdomains and simpler trial functions defined over these subdomains are used. These subdomains are called finite elements. In each finite element, the unknown quantities are approximated by means of special interpolation polynomials, the shape functions. These expansion functions have to fulfill certain conditions. They have to satisfy the continuity conditions from one element to another, e.g., the normal component of $\mathbf{B}$ and $\mathbf{D}$ or the tangential components of $\mathbf{E}$ and $\mathbf{H}$ have to be continuous, depending upon the potential formulation to be used to represent the field quantities. Elements with such shape functions are called conformal elements. The global approximation of the unknown quantities is established by means of global shape functions. These global shape functions have a local support, outside of which their value is zero.

Two types of shape functions are used in this work. They are either assigned to the nodes or to the edges of the finite element mesh. In nodal finite elements, node based scalar shape functions are used to approximate the unknown potentials and in edge finite elements, edge based vector shape functions serve this purpose.

The mapping of the geometry into curvilinear coordinate systems and the approximation of the scalar potentials is performed by means of nodal shape functions. Vector potentials can either be approximated by means of nodal finite elements, whereby each component of the vector potential is expanded using the same set of functions, or by means of edge finite elements. Edge finite elements are used in this work for vector potential expansion. A hybrid finite element with 56 degrees of freedom (DoFs), 36 edges and 20 nodes, is shown in Figure 1.1 with the order numbers assigned to the DoFs and the geometry of the finite element in a local coordinate system indicated. Second order interpolation polynomials $N_k^{(e)}$ (given in the appendix) are assigned to

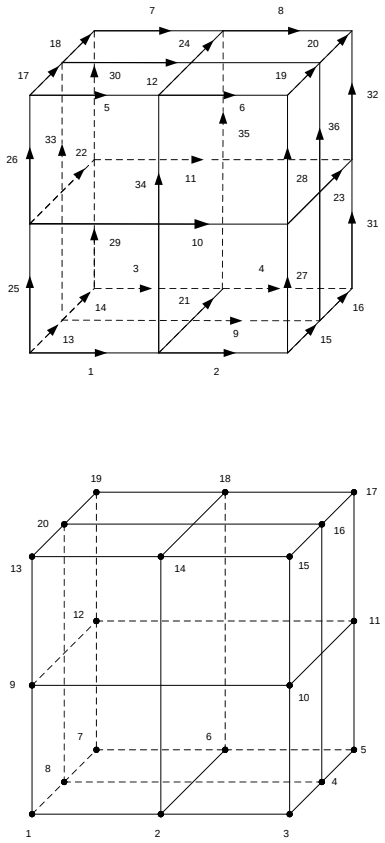

Figure 1.1 Edge elements and Nodal elements.

the nodes of a finite element with the following property:

$$N_k^{(e)} = \begin{cases} 1 & \text{in the node } k, \\ 0 & \text{in all other nodes,} \end{cases} \tag{1.25}$$

where the superscript (e) corresponds to one finite element. The corresponding global shape functions $N_k(k = 1, 2, \cdots, n_n)$ are one in the node k of the finite element mesh and zero in all other nodes, where n_n is the number of nodes in the mesh.
Similarly, second order vector polynomials $\mathbf{N}_k^{(e)}$ are assigned to the edges of the finite elements. The vector polynomial functions used in this work can be written as

$$\mathbf{N}_k^{(e)} = f_k \; grad \; \alpha, \qquad \text{with } \alpha = \xi, \eta \;\text{ or }\; \zeta, \tag{1.26}$$

where ξ, η and ζ are the axes in the local coordinate system and f_k are polynomial functions (given in appendix) corresponding to the respective edges of the finite element in the three directions. The edge shape functions $\mathbf{N}_k^{(e)}$ are further chosen to have the following property:

$$\int_{C_k} \mathbf{N}_l^{(e)} \cdot d\mathbf{s} = \begin{cases} 1 & l = k, \\ 0 & l \neq k \end{cases}, \tag{1.27}$$

where C_k stands for the k^{th} edge in the problem finite element mesh. The corresponding global shape function $\mathbf{N}_k$ $(k = 1, 2, \cdots, n_e)$ has the same property in relation with global edges where n_e is the total number of edges in the finite element mesh.
The transformation between the local and the global coordinates is established by means of locally defined nodal basis functions as

$$\begin{aligned} x(\xi, \eta, \zeta) &= \sum_{k=1}^{{n_n}^{(e)}} x_k N_k^{(e)}(\xi, \eta, \zeta), \\ y(\xi, \eta, \zeta) &= \sum_{k=1}^{{n_n}^{(e)}} y_k N_k^{(e)}(\xi, \eta, \zeta), \\ z(\xi, \eta, \zeta) &= \sum_{k=1}^{{n_n}^{(e)}} z_k N_k^{(e)}(\xi, \eta, \zeta), \end{aligned} \tag{1.28}$$

where (x_k, y_k, z_k) are the global coordinates of the node k and ${n_n}^{(e)}$ stands for the number of nodes in one element. The same transformation defines the element shape functions in terms of the global coordinates (x, y, z). The global set of expansion functions, either nodal based or edge based shape functions, are used to approximate the unknown potential functions, in the Galerkin's equations (1.18). These global expansion functions are functions of (x, y, z) and are also used to satisfy the Dirichlet boundary conditions (1.15).
Scalar potential functions can only be approximated by nodal shape functions. The following function u_D can be constructed to satisfy the Dirichlet boundary condition (1.3)

$$u_D = \sum_{k=1}^{n_D} g_k N_k. \tag{1.29}$$

where g_k is the given value of the function g in the node k and n_D is the number of nodes on the Dirichlet boundary Γ_D. Therefore the scalar potential u is approximated as

$$u^{(n)} = u_D + \sum_{k=n_D+1}^{n_n} u_k N_k. \tag{1.30}$$

Edge basis functions are used in this work for the approximation of vector potentials due to the advantage in case of iron air interfaces and the sharp corners in the problem region, although the possibility to use the nodal expansion functions is also available by approximating each component of the vector potential with the same set of the basis functions.
When vector potentials are approximated by edge basis functions, the function $\mathbf{u}_D$ satisfying (1.3) is constructed as

$$\mathbf{u}_D = \sum_{k=1}^{n_{D_e}} g_k \mathbf{N}_k, \tag{1.31}$$

where n_{D_e} stands for the number of edges on Γ_D and the scalar g_k is the line integral of the known function $\mathbf{g}$, the tangential component of the $\mathbf{u}$ specified on Γ_D. The unknown vector potential $\mathbf{u}$ can now be written as

$$\mathbf{u}^{(n)} = \mathbf{u}_D + \sum_{k=n_{D_e}+1}^{n_e} u_k \mathbf{N}_k, \tag{1.32}$$

where

$$u_k = \int_{C_k} \mathbf{u}.d\mathbf{s}. \tag{1.33}$$

It is to be noted that only vector quantities with continuous tangential components can be expanded by means of edge elements.

There exists a functional relationship between the spaces spanned by the two sets of expansion functions $\{N_k\}$ and $\{\mathbf{N}_k\}$. Let W^0 be the space spanned by the nodal basis functions with $N_k \in W^0$ and W^1 the space spanned by the edge basis functions with $\mathbf{N}_k \in W^1$, then the following functional relation holds:

$$grad(W^0) \subset W^1, \tag{1.34}$$

i.e. the gradients of the nodal basis functions lie in the same function space in which the edge basis functions [36]. It is obvious from the fact that the sum of all nodal basis functions is one

$$\sum_{k=1}^{n_n} N_k = 1 \tag{1.35}$$

so

$$\sum_{k=1}^{n_n} gradN_k = 0, \tag{1.36}$$

i.e., the maximal of number linearly independent gradients of the nodal basis functions is $(n_n - 1)$, that is the number of tree edges in the graph defined by the finite element mesh. On the other hand, the gradients of the nodal basis functions are in the function space spanned by the edge basis functions, therefore we have the following $n_n - 1$ linearly independent relations

$$grad N_k = \sum_{l=1}^{n_e} c_{kl} \mathbf{N}_l, \qquad k = 1, 2, \cdots, n_n - 1, \tag{1.37}$$

where

$$\sum_{l=1}^{n_e} c_{kl}^2 > 0, \qquad k = 1, 2, \cdots, n_n - 1. \tag{1.38}$$

By taking the curl of (1.37) one can obtain

$$\sum_{l=1}^{n_e} c_{kl}\ curl \mathbf{N}_l = \mathbf{0}, \qquad k = 1, 2, \cdots, n_n - 1. \tag{1.39}$$

The above three relations imply that the maximal number linearly independent curls of the edge basis functions is $n_e - (n_n - 1)$, the number of cotree edges in the graph of the finite element mesh. The nodal and the edge basis functions are linearly independent but not their gradients or their curls. There exist only $(n_n - 1)$ linearly independent gradients of the nodal basis functions in W^1 (i.e. equal to tree edges) and $n_e - (n_n - 1)$ linearly independent curls of the edge basis functions (i.e. equal to the number of cotree edges).

Chapter 2

Eddy Current Problems and Skin Effect Problems

An eddy current problem arises if a time varying magnetic field is excited within a body made of conducting material and the excitation field is realized by a coil with given current density $\mathbf{J}_0$ situated outside the conductor. This leads to a static but time varying magnetic field in the non-conducting regions Ω_n surrounding the eddy current carrying conductors constituting the region Ω_c ($\Omega = \Omega_n + \Omega_c$). In Ω_c, both the magnetic and the eddy current fields are present and are coupled. On the other hand, if the total current through a conductor or the applied voltage across it is given and the current density distribution is unknown then a skin effect problem is arrived at. The displacement current density is assumed to be negligible, i.e. the differential equations of quasi-static fields hold.

Skin effect problems are in fact a special class of eddy current fields described by means of partial differential equations coupled to external source voltages or currents. The prescription of the voltage or the current is the peculiarity of skin effect problems. The problem domain of eddy current or skin effect problems constitutes usually conducting parts, air regions and also ferromagnetic materials, are regions of complex geometries. Therefore the complex geometries and nonlinear material properties demand numerical techniques to be used for the solution of such problems. Finite element techniques are widely used for both of these problems. The differential equations and the boundary conditions for the field vectors for both classes are presented first and then the two problems are described separately.

2.1. Differential equations and boundary conditions for field quantities

The set of differential equations is:

$$curl\mathbf{H} = \mathbf{J} \text{ in } \Omega_c, \tag{2.1}$$

$$curl\mathbf{H} = \mathbf{J}_0 \text{ in } \Omega_n, \tag{2.2}$$

$$curl\mathbf{E} = -\frac{\partial \mathbf{B}}{\partial t} \text{ in } \Omega_c, \tag{2.3}$$

$$div\mathbf{B} = 0 \text{ in } \Omega. \tag{2.4}$$

The boundary conditions, as shown in Figs. 2.1 and 2.2,

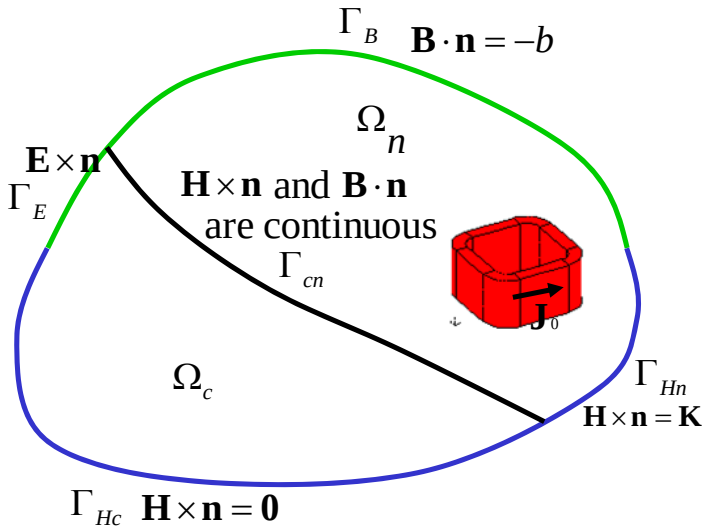

Figure 2.1 Field model of an eddy current problem

for the eddy current problem are

$$\mathbf{E}\times\mathbf{n} = \mathbf{0} \text{ on } \Gamma_E, \tag{2.5}$$

$$\mathbf{H}\times\mathbf{n} = \mathbf{0} \text{ on } \Gamma_{H_c}, \tag{2.6}$$

$$\mathbf{H}\times\mathbf{n} = \mathbf{K} \text{ on } \Gamma_{H_n}, \tag{2.7}$$

$$\mathbf{B}\cdot\mathbf{n} = -b \text{ on } \Gamma_B \tag{2.8}$$

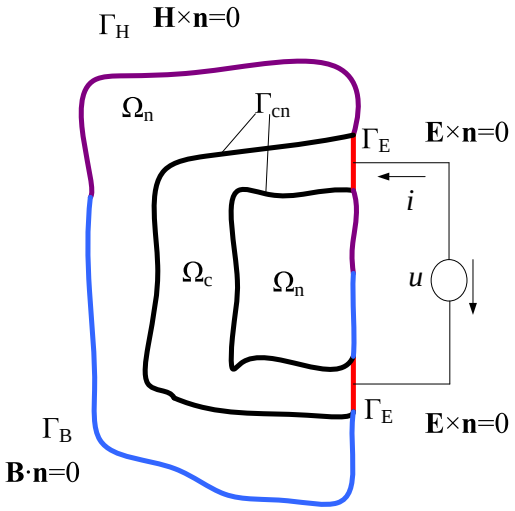

Figure 2.2 Field model of a skin effect problem

and for skin effect problems:

$$\mathbf{E} \times \mathbf{n} = \mathbf{0} \text{ on } \Gamma_E, \tag{2.9}$$

$$\mathbf{H} \times \mathbf{n} = \mathbf{0} \text{ on } \Gamma_{H_c} \textit{ and } \Gamma_{H_n}, \tag{2.10}$$

$$\mathbf{B} \cdot \mathbf{n} = 0 \text{ on } \Gamma_B \tag{2.11}$$

where $\mathbf{H}$ is the magnetic field intensity, $\mathbf{J}$ the current density vector, $\mathbf{E}$ the electric field intensity, $\mathbf{B}$ the magnetic flux density and the subscripts c and n represent the conducting and the non-conducting regions respectively. $\mathbf{J}_0$ is the given current density of the coils which is supposed to be known. $\mathbf{n}$ is the unit normal vector pointing outward from the problem domain Ω.
Additionally, the material equations can be written as:

$$\mathbf{H} = \nu\mathbf{B} \text{ or } \mathbf{B} = \mu\mathbf{H}, \tag{2.12}$$

$$\mathbf{J} = \sigma\mathbf{E} \text{ or } \mathbf{E} = \rho\mathbf{J} \tag{2.13}$$

where ν is the reluctivity, μ the permeability, ρ the resistivity and σ the conductivity. The interface conditions for the magnetic field intensity in the eddy current domain $\mathbf{H}_c$ and in the eddy current free domain $\mathbf{H}_n$, and the magnetic flux density in the eddy current domain $\mathbf{B}_c$ and in the eddy current free domain $\mathbf{B}_n$ are:

$$\mathbf{H}_c \times \mathbf{n}_c + \mathbf{H}_n \times \mathbf{n}_n = \mathbf{0} \text{ on } \Gamma_{cn}, \tag{2.14}$$

$$\mathbf{B}_c \cdot \mathbf{n}_c + \mathbf{B}_n \cdot \mathbf{n}_n = 0 \text{ on } \Gamma_{cn}. \tag{2.15}$$

where $\mathbf{n}_c$ is a unit normal vector pointing from eddy current domain towards the eddy current free domain and $\mathbf{n}_n$, the unit normal vector pointing from non-conducting towards the conducting domain on the interface of the two regions which is represented by Γ_{cn}.

2.2. Eddy current problem

The finite element solution of the field boundary value problem is usually sought with the introduction of potential functions [6, 11]. There are basically two possibilities to choose the potential functions describing eddy current problems.
In a finite element context, the vector potentials are advantageously approximated by edge basis functions whereas the scalar potentials should be expanded by node based ones.

2.2.1. $\mathbf{A}, v - \mathbf{A}$ formulation

The $\mathbf{A}, v - \mathbf{A}$ formulation uses the magnetic vector potential $\mathbf{A}$ introduced in the entire problem domain and additionally, the time integrated electric scalar potential v is defined in the eddy current region only.

$$\mathbf{B} = curl\mathbf{A} \text{ in } \Omega, \tag{2.16}$$

$$\mathbf{E} = -\frac{\partial \mathbf{A}}{\partial t} - grad\frac{\partial v}{\partial t} \text{ in } \Omega_c. \tag{2.17}$$

This results in the exact satisfaction of (2.3) and (2.4). To obtain a symmetric system, the scalar potential V in terms of the time derivative of a modified scalar potential v i.e.,

$$V = \frac{\partial v}{\partial t}, v(t=0) = 0 \text{ or } v = \int_0^t V(\mathbf{r}, \tau) d\tau, \tag{2.18}$$

is introduced.

2.2.1.1. Boundary value problem for the potentials

(2.1) and (2.2) respectively, can be written in terms of potential functions using (2.16), (2.17) and the fist part of the material relation (2.12)

$$curl(\nu curl\mathbf{A}) + \sigma\frac{\partial\mathbf{A}}{\partial t} + \sigma grad\frac{\partial v}{\partial t} = \mathbf{0} \text{ in } \Omega_c, \tag{2.19}$$

$$curl(\nu curl\mathbf{A}) = \mathbf{J}_0 \text{ in } \Omega_n. \tag{2.20}$$

In the eddy current domain, there is one equation for two potential functions, a second scalar differential equation can be obtained from the law of continuity $div\mathbf{J}_c = 0$, which is in fact the consequence of (2.1), as

$$div(-\sigma\frac{\partial\mathbf{A}}{\partial t} - \sigma grad\frac{\partial v}{\partial t}) = 0 \text{ in } \Omega_c. \tag{2.21}$$

The complete boundary value problem in terms of potential functions, using an ungauged vector potential, consists of the differential equations (2.19), (2.20), (2.21) and the boundary conditions:

According to (2.6) the tangential component of $\mathbf{H}$ is zero on Γ_{H_c} that implies normal component of $\mathbf{J}$ also vanishes on this boundary part. So in terms of the potential functions,

$$\nu curl\mathbf{A} \times \mathbf{n} = \mathbf{0} \text{ and}$$
$$\mathbf{n} \cdot (-\sigma\frac{\partial\mathbf{A}}{\partial t} - \sigma grad\frac{\partial v}{\partial t}) = 0 \text{ on } \Gamma_{H_c}. \tag{2.22}$$

(2.5) implies

$$\mathbf{n} \times \mathbf{A} = \mathbf{0} \text{ and } v = constant = v_0 \text{ on } \Gamma_E \tag{2.23}$$

According to (2.7) the known surface current density $\mathbf{K}$ is given as the tangential component of $\mathbf{H}$ on Γ_{H_n}, so

$$\nu curl\mathbf{A} \times \mathbf{n} = \mathbf{K} \text{ on } \Gamma_{H_n} \tag{2.24}$$

The magnetic surface charge density b in (2.8) is specified in terms of the tangential component of $\mathbf{A}$ as

$$\mathbf{n} \times \mathbf{A} = \alpha \text{ on } \Gamma_B \tag{2.25}$$

The continuity condition of the normal component of $\mathbf{B}$ in (2.15) is written as

$$curl\mathbf{A} \cdot \mathbf{n}_c + curl\mathbf{A} \cdot \mathbf{n}_n = 0 \text{ on } \Gamma_{cn}, \tag{2.26}$$

The continuity condition of the tangential component of $\mathbf{H}$ in (2.14) in terms of the potential functions is

$$\nu_c curl\mathbf{A} \times \mathbf{n}_c + \nu_n curl\mathbf{A} \times \mathbf{n}_n = \mathbf{0} \text{ on } \Gamma_{cn}, \tag{2.27}$$

$$\mathbf{n}_c \cdot \sigma\frac{\partial}{\partial t}(\mathbf{A} + gradv) = 0 \text{ on } \Gamma_{cn}. \tag{2.28}$$

2.2.1.2. Galerkin equations

The use of the edge basis functions for the expansion of vector potential ensures the continuity of its tangential component on Γ_{cn}. Consequently, the continuity of the normal component of the magnetic flux density $\mathbf{B}$ (2.15) and, thus (2.26) is automatically ensured. The only concern which remains for the interface condition, is the tangential continuity of the magnetic field intensity $\mathbf{H}$. That is also achieved in the weak sense naturally by the surface integrals of the form

$$\int_{\Gamma_{cn}} \mathbf{N}_i \cdot (\mathbf{H} \times \mathbf{n}) \; d\Gamma. \tag{2.29}$$

arising in the Galerkin equations both in Ω_n and Ω_c and thus canceling out.

The vector potential is approximated by edge basis functions as

$$\mathbf{A} \approx \mathbf{A}_h = \sum_{j=1}^{n_1} A_j \mathbf{N}_j \tag{2.30}$$

where n_1 is the number of edges in the finite element mesh except those on Γ_E and Γ_B, and A_j are the line integrals of $\mathbf{A}$ along the edges.

The electric scalar potential is expanded by nodal basis functions as

$$v \approx v_h = \sum_{j=1}^{n_2} v_j N_j \tag{2.31}$$

where n_2 is the number of nodes in Ω_c except those on Γ_E and v_j are the nodal values of the approximated scalar potential.
Setting (2.30) and (2.31) into (2.19), (2.20) as well as into the vector Neumann boundary condition in (2.22) and (2.24) and using the basis functions $\mathbf{N}_i$ as weighting functions for vector equations, results into the equations

$$\begin{aligned} \int_{\Omega_c} \mathbf{N}_i \cdot \left[curl(\nu curl \mathbf{A}_h) + \sigma \frac{\partial}{\partial t}(\mathbf{A}_h + grad v_h) \right] \; d\Omega \\ + \int_{\Gamma_{H_c}} \mathbf{N}_i \cdot (\nu curl \mathbf{A}_h \times \mathbf{n}) \; d\Gamma + \int_{\Omega_n} \mathbf{N}_i \cdot curl(\nu curl \mathbf{A}_h) \; d\Omega \\ + \int_{\Gamma_{H_n}} \mathbf{N}_i \cdot (\nu curl \mathbf{A}_h \times \mathbf{n}) \; d\Gamma + \int_{\Gamma_{cn}} \mathbf{N}_i \cdot (\nu_c curl \mathbf{A}_h \times \mathbf{n}_c) \; d\Gamma \\ + \int_{\Gamma_{cn}} \mathbf{N}_i \cdot (\nu_n curl \mathbf{A}_h \times \mathbf{n}_n) \; d\Gamma = \int_{\Omega_n} \mathbf{N}_i \cdot \mathbf{J}_0 \; d\Omega + \int_{\Gamma_{H_n}} \mathbf{N}_i \cdot \mathbf{K} \; d\Gamma, \\ (i = 1, 2, \cdots, n_1), \end{aligned} \tag{2.32}$$

which can be transformed, using integration by parts (i.e. considering the vector identities, $\mathbf{F} \cdot curl\, \mathbf{G} = \mathbf{G} \cdot curl\, \mathbf{F} - div\, (\mathbf{F} \times \mathbf{G})$ and $f\, div\, \mathbf{F} = -\mathbf{F} \cdot grad\, f + div\, (f\mathbf{F})$)

and taking into account that the coordinate functions fulfill the homogeneous Dirichlet boundary conditions and also making use of the divergence theorem, into the following Galerkin equations:

$$\int_{\Omega_c} curl\mathbf{N}_i \cdot \nu curl\mathbf{A}_h \, d\Omega + \int_{\Omega_c} \mathbf{N}_i \cdot \sigma \frac{\partial}{\partial t} \left(\mathbf{A}_h + grad\ v_h\right)\ d\Omega = \int_{\Omega_c} \mathbf{N}_i \cdot \mathbf{J}_0 \, d\Omega + \int_{\Gamma_{Hn}} \mathbf{N}_i \cdot \mathbf{K} \, d\Omega \quad i = 1, 2, \cdots, n_1. \tag{2.33}$$

Setting (2.30) and (2.31) into (2.21) as well as into the scalar Neumann boundary condition in (2.22) and using the basis functions N_i as weighting functions for scalar equations, results into the equations

$$\int_{\Omega_c} N_i \left[-div\sigma \frac{\partial}{\partial t} \left(\mathbf{A}_h + gradv_h\right)\right]\ d\Omega + \int_{\Gamma_{Hc}} N_i \left[\sigma \frac{\partial}{\partial t} \mathbf{n} \cdot \left(\mathbf{A}_h + gradv_h\right)\right]\ d\Gamma + \int_{\Gamma_{cn}} N_i \left[\sigma \frac{\partial}{\partial t} \mathbf{n} \cdot \left(\mathbf{A}_h + gradv_h\right)\right]\ d\Gamma = 0, \quad (i = 1, 2, \cdots, n_2), \tag{2.34}$$

and the similar transformation as used above gives the following Galerkin equations:

$$\int_{\Omega_c} gradN_i \cdot \sigma \frac{\partial}{\partial t} \left(\mathbf{A}_h + gradv_h\right)\ d\Omega = 0, \quad i = 1, 2, \cdots, n_2. \tag{2.35}$$

It has been shown in section 1.3 that the resulting system of equations is singular, therefore the consistency of the right hand side is mandatory. This is achieved by the introduction of an impressed current vector potential $\mathbf{T}_0$ to represent the effect of the coils with given current density. The function $\mathbf{T}_0$ satisfies:

$$curl\mathbf{T}_0 = \mathbf{0} \quad \text{in } \Omega_c, \quad \text{and} \quad curl\mathbf{T}_0 = \mathbf{J} - 0 \quad \text{in } \Omega_n, \tag{2.36}$$

$$\mathbf{T}_0 \times \mathbf{n} = \mathbf{K} \quad \text{on } \Gamma_{H_n}, \quad \text{and} \quad \mathbf{T}_0 \times \mathbf{n} = \mathbf{0} \quad \text{on } \Gamma_{H_c}. \tag{2.37}$$

The above introduction results in the consistent right hand side of the equation (2.33) as

$$\int_{\Omega_c} curl\mathbf{N}_i \cdot \nu curl\mathbf{A}_h \, d\Omega + \int_{\Omega_c} \mathbf{N}_i \cdot \sigma \frac{\partial}{\partial t} \left(\mathbf{A}_h + grad\ v_h\right)\ d\Omega = \int_{\Omega_c} curl\mathbf{N}_i \cdot \mathbf{T}_0 \, d\Omega \quad i = 1, 2, \cdots, n_1. \tag{2.38}$$

2.2.2. $\mathbf{T}, \Phi - \Phi$ formulation

In this formulation, the current vector potential $\mathbf{T}$ is introduced in the conducting domain and a magnetic scalar potential Φ is used in the both eddy current as well as in the eddy current free domain to determine the electromagnetic field quantities in the problem domain.

The field quantities are derived from the potentials as

$$\mathbf{H} = \mathbf{T}_0 + \mathbf{T} - grad\Phi, \quad \mathbf{J} = curl\mathbf{T}_0 + curl\mathbf{T} \quad \text{in } \Omega_c, \tag{2.39}$$

$$\mathbf{H} = \mathbf{T}_0 - grad\Phi, \quad \mathbf{J} = curl\mathbf{T}_0 \quad \text{in } \Omega_n, \tag{2.40}$$

Ampere's law (2.1) and (2.2) is, hence, satisfied exactly with the above assumption.

2.2.2.1. Boundary value problem for the potentials

Faraday's law (2.3) leads to the differential equation

$$curl\left(\rho curl\mathbf{T}\right) + \frac{\partial}{\partial t}\mu\left(\mathbf{T} - grad\Phi\right) = -curl\left(\rho curl\mathbf{T}_0\right) - \frac{\partial}{\partial t}\left(\mu\mathbf{T}_0\right) \quad \text{in } \Omega_c. \tag{2.41}$$

In the eddy current domain, there is one equation for two potential functions, a second scalar differential equation can be obtained from the divergence free property of the time derivative of the magnetic flux density $\mathbf{B}$, which is a consequence of (2.3):

$$div\,\frac{\partial}{\partial t}\left[\mu\left(\mathbf{T} - grad\Phi\right)\right] = -div\left(\mu\mathbf{T}_0\right) \quad \text{in } \Omega_c, \tag{2.42}$$

similarly in the eddy current free domain,

$$-\,div\,\frac{\partial}{\partial t}\left(\mu grad\Phi\right) = -div\left(\mu\mathbf{T}_0\right) \quad \text{in } \Omega_n. \tag{2.43}$$

The complete boundary value problem in terms of potential functions, using an ungauged vector potential, consists of the differential equations (2.41), (2.42), (2.43) and the boundary conditions, in (2.5), (2.6), (2.8) and (2.7) respectively, in terms of the potential functions:

$$\begin{aligned} \rho curl\mathbf{T} \times \mathbf{n} &= -\rho curl\mathbf{T}_0 \times \mathbf{n}\,(=\mathbf{0}) \text{ and} \\ \mathbf{n} \cdot \mu\left(\mathbf{T} - grad\Phi\right) &= -\mathbf{T}_0 \cdot \mathbf{n}\,(=0) \text{ on } \Gamma_E, \end{aligned} \tag{2.44}$$

$$\mathbf{T} \times \mathbf{n} = \mathbf{T}_0 \times \mathbf{n}\,(=\mathbf{0}) \quad \text{and} \quad \Phi = \Phi_0 \text{ on } \Gamma_{H_c}, \tag{2.45}$$

$$\mathbf{n} \cdot \mu grad\Phi = \mu \frac{\partial \Phi}{\partial n} = b + \mu \mathbf{T}_0 \cdot \mathbf{n} \quad \text{on } \Gamma_B, \tag{2.46}$$

$$\mathbf{T}_0 \times \mathbf{n} = \mathbf{K}, \quad \Phi = \Phi_0 \quad \text{on } \Gamma_{H_n}, \tag{2.47}$$

2.2.2.2. Galerkin equations

The continuity of the tangential component of the magnetic field intensity, i.e. of $\mathbf{H} \times \mathbf{n}$ is ensured by the continuity of the magnetic scalar potential in the two domains and by setting the tangential component of the current vector potential to zero on the interface:

$$\mathbf{T} \times \mathbf{n} = \mathbf{0} \quad \text{on } \Gamma_{cn}. \tag{2.48}$$

The continuity of the normal component of the magnetic flux density $\mathbf{B}$ is also achieved in the weak sense through surface integrals of the form

$$\int_{\Gamma_{cn}} N_i \, \mathbf{B} \cdot \mathbf{n} \, d\Gamma \tag{2.49}$$

arising in the Galerkin equations both in Ω_n and Ω_c and thus canceling out.

The vector potential is approximated by edge basis functions as

$$\mathbf{T} \approx \mathbf{T}_h = \sum_{j=1}^{n_1} T_j \mathbf{N}_j, \tag{2.50}$$

where n_1 is the number of edges in the eddy current domain except those on Γ_H and Γ_{cn}, and T_j are the line integrals of $\mathbf{T}$ along the edges.

The magnetic scalar potential is expanded by nodal basis functions as

$$\Phi \approx \Phi_h = \sum_{j=1}^{n_2} \Phi_j N_j. \tag{2.51}$$

where n_2 is the number of nodes in Ω_c except those on Γ_E and v_j are the nodal values of the approximated scalar potential.

Setting (2.50) and (2.51) into (2.41) as well as into the vector Neumann boundary condition in (2.44) and using the basis functions $\mathbf{N}_i$ as weighting functions for vector equation, results into the equations

$$\int_{\Omega_c} \mathbf{N}_i \cdot \, curl\left(\rho curl \mathbf{T}_h\right) \, d\Omega$$
$$+ \int_{\Omega_c} \mathbf{N}_i \cdot \left[\frac{\partial}{\partial t}\left(\mu \mathbf{T}_h\right) - \frac{\partial}{\partial t}\left(\mu grad\Phi_h\right)\right] \, d\Omega + \int_{\Gamma_E} \mathbf{N}_i \cdot \left(\rho curl \mathbf{T}_h \times \mathbf{n}\right) \, d\Gamma$$
$$= -\int_{\Omega_c} \mathbf{N}_i \cdot \left[curl\left(\rho curl \mathbf{T}_0\right) + \frac{\partial}{\partial t}\left(\mu \mathbf{T}_0\right)\right] \, d\Omega, \quad i = 1, 2, \cdots, n_1, \tag{2.52}$$

which can be transformed, by using partial integration, into the following Galerkin equations:

$$\int_{\Omega_c} curl \mathbf{N}_i \cdot \rho curl \mathbf{T}_h \, d\Omega + \int_{\Omega_c} \mu \frac{\partial}{\partial t}\left(\mathbf{T}_h - grad\Phi_h\right) \, d\Omega$$
$$= -\int_{\Omega_c} curl \mathbf{N}_i \cdot \rho curl \mathbf{T}_0 \, d\Omega - \int_{\Omega_c} \mathbf{N}_i \cdot \frac{\partial}{\partial t}\left(\mu \mathbf{T}_0\right) \, d\Omega \quad i = 1, 2, \cdots, n_1 \tag{2.53}$$

and, setting (2.50) and (2.51) into (2.42), (2.43) and as well as into the scalar Neumann boundary condition in (2.44) and (2.46) and using the basis functions N_i as weighting functions for scalar equations, results into the equations

$$\int_{\Omega_c} N_i \frac{\partial}{\partial t} div\left[\left(\mu \mathbf{T}_h - \mu grad\Phi_h\right)\right] \, d\Omega - \int_{\Omega_n} N_i \frac{\partial}{\partial t} div\left(\mu grad\Phi_h\right) \, d\Omega$$
$$+ \int_{\Gamma_E} N_i \frac{\partial}{\partial t} \mu \left(-\mathbf{T}_h \cdot \mathbf{n} + \frac{\partial \Phi_h}{\partial n}\right) \, d\Gamma + \int_{\Gamma_B} N_i \frac{\partial}{\partial t}\left(\frac{\partial \Phi_h}{\partial n}\right) \, d\Gamma$$
$$+ \int_{\Gamma_{cn}} N_i \left[-\frac{\partial}{\partial t}\left(\mu \mathbf{T}_h \cdot \mathbf{n}_c\right) + \frac{\partial}{\partial t}\left(\mu \frac{\partial \Phi_h}{\partial n_c}\right) + \frac{\partial}{\partial t}\left(\mu \frac{\partial \Phi_h}{\partial n_n}\right)\right]$$
$$= -\int_{\Omega} N_i \frac{\partial}{\partial t} div\left(\mu \mathbf{T}_0\right) \, d\Omega + \int_{\Gamma_B} N_i \frac{\partial}{\partial t}\left(b + \mu \mathbf{T}_0 \cdot \mathbf{n}\right) \, d\Gamma$$
$$+ \int_{\Gamma_{cn}} N_i \frac{\partial}{\partial t}\left(\mu \mathbf{T}_0 \cdot \mathbf{n}_c + \mu \mathbf{T}_0 \cdot \mathbf{n}_n\right) \, d\Gamma \quad i = 1, 2, \cdots, n_2, \tag{2.54}$$

which can be transformed, by using partial integration, into the following Galerkin equations:

$$-\int_{\Omega} gradN_i \cdot \frac{\partial}{\partial t} \, \mu grad\Phi_h \, d\Omega$$
$$+ \int_{\Omega_c} gradN_i \cdot \frac{\partial}{\partial t} \, \left(\mu \mathbf{T}_h\right) \, d\Omega$$
$$= -\int_{\Omega} gradN_i \cdot \frac{\partial}{\partial t} \, \left(\mu \mathbf{T}_0\right) - \int_{\Gamma_B} N_i \frac{\partial b}{\partial t} \, d\Omega \quad i = 1, 2, \cdots, n_2. \tag{2.55}$$

2.3. Skin effect problems

The devices encountering eddy currents are usually supplied through electric circuits. The currents and voltages associated with the conducting parts of those appliances are normally required to be coupled with the circuits. The field model of a general skin effect problem along with the boundary and interface conditions, as shown in Fig. 2.2 is presented here with a brief introduction of the two global conditions to be treated separately in the next four chapters.
It involves an eddy current carrying domain Ω_c surrounded by a non-conducting region $\Omega_n(\Omega{=}\Omega_c{+}\Omega_n)$. The electric and magnetic fields are coupled in the conducting domain only, while in the non-conducting domain the magnetic field is essentially static [37].

The same potential introduction as used for the eddy current problems is applicable in skin effect problems too. The two global conditions, i.e. voltage and current prescription related to external sources are to be incorporated in case of skin effect problems. Boundary conditions for the potential functions, which arise in case of the prescribed voltage and current, are different for the four possible cases.

2.3.1. Voltage excitation condition

In the $\mathbf{A}, v-\mathbf{A}$ formulation the given voltage condition is to be incorporated in terms of the modified electric scalar potential on the boundary parts where tangential component of the electric field vanishes, i.e. on the electrodes. This treatment will be shown in the following chapter.

In the $\mathbf{T}, \Phi-\Phi$ formulation, the condition of voltage prescription is treated by introducing an additional current vector potential the so called source field function $\mathbf{t}_0$. The properties of this function and the additional equations arising in the system of equations are arrived at in the *chapter 5*.

2.3.2. Current excitation condition

Skin effect problems with the given current condition are easily handled with the $\mathbf{T}, \Phi-\Phi$ formulation provided the eddy current domain is simply connected. The impressed field function $\mathbf{T}_0$ is used to incorporate this condition, with the assumption of arbitrary current filament of known current between the two source electrodes and running solely in the conducting domain. The role of the impressed field function and its properties are different from those of the same function used in the eddy current problem. This will be presented in *chapter 4*.

If the currents instead of voltages are specified for the electromotive sources of the skin effect problem then the Dirichlet boundary condition for the $\mathbf{A}, v-\mathbf{A}$ formulation

in the conducting regions becomes unspecified. This will be treated similarly to periodic boundary conditions. This is achieved by the introduction of a sum nodal basis function corresponding to the nodes on each of the electrodes with the prescribed current by setting the scalar potential to an unknown constant on that specific electrode. The approach to obtain this function and its properties are described in *chapter 6*. The new basis function is then used as a weighting function to obtain the additional equations. The relation between this coordinate function and the prescribed current, in terms of both the vector and scalar potential functions, is shown and the complete set of Galerkin equations is also derived in *chapter 6*.

Chapter 3

$\mathbf{A}, v - \mathbf{A}$ Formulation of Skin Effect Problems with Voltage Excitation

In this formulation, the Dirichlet boundary conditions on the electrodes are non homogeneous. The prescribed voltage condition, in terms of the modified electric scalar potential v, is the essential boundary condition to be satisfied. It is shown that the scalar potential realizes a strong global constraint which appears in the set of Galerkin equations obtained in this formulation.

The problem consisting of n thick inductors shown in Fig.3.1 is used to arrive at the formulation. It can be assumed that the normal component of the magnetic flux density vanishes at a reasonably long distance from the magnetic field sources, i.e. from the electric currents and the permanent magnets. Hence, there is an option always available to assume a boundary surface away from the problem domain where homogeneous conditions for the normal component of magnetic flux density can be defined. This kind of boundary is termed as the far boundary and is denoted by Γ_0 here.

3.1. Strong global constraint for the $\mathbf{A}, v - \mathbf{A}$ formulation

The voltage is a strong global constraint in this formulation [38]. If the voltage is prescribed, it is to be satisfied as an essential boundary condition for the scalar potential on the electrodes connected to the voltage sources. In this situation, the boundary condition for the potential functions is

$$\mathbf{A} \times \mathbf{n} = \mathbf{0},\ v^i(t) = \int_0^t u^i(\tau) d\tau \text{ on } \Gamma_E^i \quad \text{for} \quad i = 1, 2, \cdots, n \tag{3.1}$$

$$\mathbf{A} \times \mathbf{n} = \mathbf{0},\ v^i(t) = 0 \text{ on } \Gamma_E^0, \text{ the reference electrode} \tag{3.2}$$

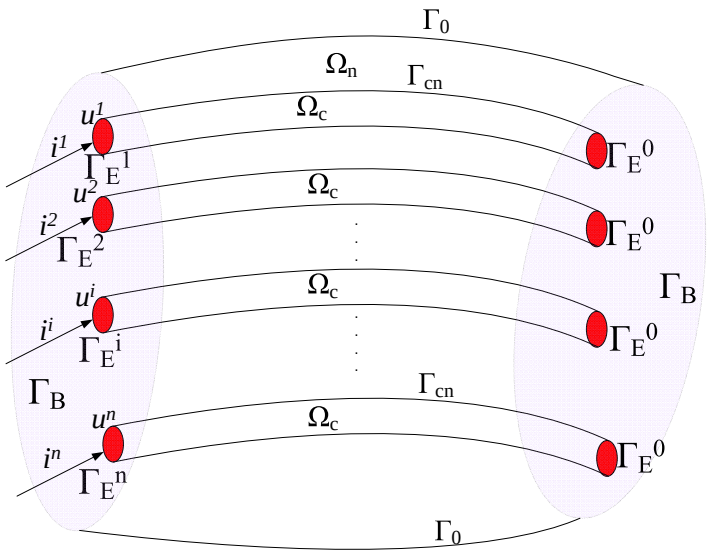

Figure 3.1 Bounded problem domain containing n conductors.

as shown in Fig.3.1. In the above two conditions, the assertion is made that the voltage is the difference of the electric scalar potential values on the two electrodes connected to the source. In order to make it explicit, the way in which the voltage is defined is important. If the voltage is defined as a line integral of the electric field intensity, $\mathbf{E}$ from one electrode to the other, i.e.

$$u(t) = \int_C \mathbf{E} \cdot d\mathbf{l}, \tag{3.3}$$

then the selection of the curve, C affects the value of the integral because of the presence of the time varying magnetic field. Another definition of the voltage is required here to be complied completely by this potential prescription on the electrodes [39]. According to this definition, the total power in the problem domain defined as the sum of the power loss and the time derivative of the magnetic energy is equal to the product of the voltage and the total current.

The total power of the arrangement is

$$p(t) = \int_{\Omega_c} \frac{|\mathbf{J}(\mathbf{r},t)|^2}{\sigma}\, d\Omega + \frac{d}{dt}\int_{\Omega_c+\Omega_n}\left(\int_0^{B(\mathbf{r},t)} H dB\right) d\Omega$$
$$= \int_{\Omega_c} \mathbf{E}\cdot\mathbf{J}\, d\Omega + \int_{\Omega_c+\Omega_n} \frac{\partial \mathbf{B}}{\partial t}\cdot\mathbf{H}\, d\Omega. \tag{3.4}$$

The second term in the above relation can be written in terms of the magnetic vector potential, $\mathbf{A}$ as

$$\int_{\Omega_c+\Omega_n} \frac{\partial \mathbf{B}}{\partial t}\cdot\mathbf{H}\, d\Omega = \int_{\Omega_c+\Omega_n} curl\frac{\partial \mathbf{A}}{\partial t}\cdot\mathbf{H}\, d\Omega \tag{3.5}$$

By using the vector identity, $div(\mathbf{A}\times\mathbf{B}) = \mathbf{B}\cdot curl\mathbf{A} - \mathbf{A}\cdot curl\mathbf{B}$ and the divergence theorem, this can be written as

$$\int_{\Omega_c+\Omega_n} curl\frac{\partial \mathbf{A}}{\partial t}\cdot\mathbf{H}\, d\Omega = \int_{\Omega_c+\Omega_n} \frac{\partial \mathbf{A}}{\partial t}\cdot curl\mathbf{H}\, d\Omega + \oint_{\partial(\Omega_c+\Omega_n)}\left(\frac{\partial \mathbf{A}}{\partial t}\times\mathbf{H}\right)\cdot\mathbf{n}\, d\Gamma. \tag{3.6}$$

On Γ_E^i, Γ_E^0, Γ_B and Γ_0, the homogeneous Dirichlet boundary condition is ensured for the magnetic vector potential, i.e. the tangential component of $\mathbf{A}$ is zero there, whereas $\mathbf{H}\times\mathbf{n}$ is zero on Γ_H, a naturally satisfied boundary condition for the potential functions. Therefore, the closed surface integral in (3.6) is overall zero,

$$\int_{\Omega_c+\Omega_n} \frac{\partial \mathbf{B}}{\partial t}\cdot\mathbf{H}\, d\Omega = \int_{\Omega_c} \frac{\partial \mathbf{A}}{\partial t}\cdot\mathbf{J}\, d\Omega. \tag{3.7}$$

Substituting (3.7) into (3.4) leads to

$$p(t) = \int_{\Omega_c}\left(\mathbf{E} + \frac{\partial \mathbf{A}}{\partial \mathbf{t}}\right)\cdot\mathbf{J} d\Omega = -\int_{\Omega_c} grad\frac{\partial v}{\partial t}\cdot\mathbf{J}\, d\Omega$$
$$= \int_{\Omega_c}\frac{\partial v}{\partial t} div\mathbf{J}\, d\Omega - \oint_{\partial\Omega_c}\frac{\partial v}{\partial t}\mathbf{J}\cdot\mathbf{n}\, d\Omega. \tag{3.8}$$

The volume integral is zero due to the divergence free property of the current density, $\mathbf{J}$ while the surface integral is also zero except on Γ_E^i because the scalar potential is set to zero on Γ_E^0 and the normal component of $\mathbf{J}$ is zero on the interface of conducting and non-conducting domains, Γ_{cn}. Hence, in view of (3.1), the above relation is simplified to

$$p(t) = -u(t)\int_{\Gamma_E^i}\mathbf{J}\cdot\mathbf{n} d\Gamma = u^i(t)i^i(t), \tag{3.9}$$

which verifies the assertion made.

3.2. Boundary value problem

The boundary value problem comprises the differential equations (2.19), (2.20), (2.21) in terms of potential functions and the boundary conditions (2.17), (2.18) and:

A Neumann boundary condition is specified on Γ_H, a symmetry plane in most of the cases

$$\nu curl\mathbf{A} \times \mathbf{n} = \mathbf{0} \text{ on } \Gamma_{H_n}, \tag{3.10}$$

$$\begin{gathered} \nu curl\mathbf{A} \times \mathbf{n} = \mathbf{0} \text{ and} \\ \mathbf{n} \cdot -\sigma \frac{\partial}{\partial t} (\mathbf{A} + grad v) = 0 \text{ on } \Gamma_{H_c} \end{gathered} \tag{3.11}$$

and a Dirichlet boundary condition on Γ_B and on Γ_0

$$\mathbf{n} \times \mathbf{A} = \mathbf{0} \text{ on } \Gamma_B \text{ and on } \Gamma_0. \tag{3.12}$$

The prescribed voltage in terms of scalar potential (3.1) is the only essential non homogeneous boundary condition to be satisfied on each of the source electrodes Γ_E^i.

3.3. Galerkin equations

To obtain the Galerkin's equations in the entire problem domain, the potential approximation is

$$\begin{aligned} \mathbf{A} \approx \mathbf{A}_h &= \sum_{j=1}^{n_1} A_j \mathbf{N}_j, \\ v \approx v_h &= v_D + \sum_{j=1}^{n_2} v_j N_j, \end{aligned} \tag{3.13}$$

whereas the same ansatz for the vector potential in eddy current domain and in the eddy current free domain is applied. The functions $\mathbf{N}_j (j = 1, 2, \cdots, n_1)$ are the edge basis functions corresponding to all the edges in both Ω_c and Ω_n except those located on Γ_E or on Γ_B [40]. At the same time, $N_j (j = 1, 2, \cdots, n_2)$ are the nodal basis functions corresponding to all the nodes in the eddy current domain which are not located on Γ_E. Thereby, the continuity of the tangential component of the vector potential is guaranteed. The coordinate functions $\mathbf{N}_j (j = 1, 2, \cdots, n_1)$ and $N_j (j = 1, 2, \cdots, n_2)$ comply with the homogenous Dirichlet boundary conditions:

$$\mathbf{n} \times \mathbf{N}_j = \mathbf{0} \text{ on } \Gamma_E \text{ and on } \Gamma_B, \; N_j = 0 \quad \text{on } \Gamma_E. \tag{3.14}$$

Furthermore, the known function v_D corresponding to Dirichlet boundary condition of the scalar potential is

$$v_D = \sum_{i=1}^{n} v_0^i \sum_{Nodes_j \in \Gamma_E^i} N_j^i, \tag{3.15}$$

Galerkin's equations are written as

$$\int_{\Omega} curl\mathbf{N}_i \cdot \nu curl\mathbf{A}_h \, d\Omega + \int_{\Omega_c} \mathbf{N}_i \cdot \sigma \frac{\partial}{\partial t} \left(\mathbf{A}_h + grad v_h\right) \, d\Omega = 0 \quad i = 1, 2, \cdots, n_1, \tag{3.16}$$

$$\int_{\Omega_c} gradN_i \cdot \sigma \frac{\partial}{\partial t} \left(\mathbf{A}_h + grad v_h\right) \, d\Omega = 0, \quad i = 1, 2, \cdots, n_2. \tag{3.17}$$

Chapter 4

$\mathbf{T}, \Phi - \Phi$ Formulation of Skin Effect Problems with Current Excitation

In the $\mathbf{T}, \Phi - \Phi$ formulation, the given current condition is incorporated by introducing the impressed field function $\mathbf{T}_0$ with different properties than that of the same function representing the effect of coils in the eddy current problem. This formulation is obtained for the skin effect problems with simply connected eddy current domain. The problem consisting of n thick inductors shown in Fig.3.1 is used to arrive at the formulation.

The unknown current vector potential $\mathbf{T}$ is introduced [41] in the eddy current domain and the reduced magnetic scalar potential Φ in the whole problem domain. The field quantities are obtained as

$$\mathbf{H} = \mathbf{T}_0 + \mathbf{T} - grad\Phi \ \text{ in } \Omega_c, \tag{4.1}$$

$$\mathbf{H} = \mathbf{T}_0 - grad\Phi \ \text{ in } \Omega_n, \tag{4.2}$$

$$\mathbf{J} = curl\mathbf{T}_0 + curl\mathbf{T} \ \text{ in } \Omega_c. \tag{4.3}$$

Both the functions $\mathbf{T}$ and $\mathbf{T}_0$ are approximated with the aid of edge basis functions $\mathbf{N}_j$, whereas the function Φ with nodal basis functions N_j. The curl of the function $\mathbf{T}_0$ is required to represent an arbitrary current density distribution in the conductors with the given net current in other words it describes the static current field. Furthermore, the tangential component of $\mathbf{T}_0$ is continuous in the whole problem region.

4.1. Strong global constraint for the $\mathbf{T}, \Phi - \Phi$ formulation

In this formulation, the total electric current is a global quantity which is directly connected with the magnetic field, $\mathbf{H}$ through Ampere's law (2.1) which is exactly

satisfied in this formulation as shown in Section 2.2.2

$$curl\mathbf{H} = \mathbf{J} \text{ and } \int_{\Gamma_{E^i}} \mathbf{J} \cdot \mathbf{n}\, ds = i^i. \tag{4.4}$$

Therefore, the total current is the strong global quantity or a strong global constraint in case it is prescribed.
In the finite element context, it can be interpreted in another way. Since, the current vector potentials $\mathbf{T}$ and $\mathbf{T}_0$ are expanded with edge basis functions, their circulation along a closed path can be directly obtained from the expansion coefficients. Therefore the flux of their curls which is current, is directly connected with these coefficients and, hence, can be said to be expressed in a strong sense.

4.2. Boundary value problem

The problem is solved in two steps, first to solve a static current flow problem to compute the function $\mathbf{T}_0$. The curl of which describes the static current field in the conducting domain. In the next step the boundary value problem for $\mathbf{T}$ and Φ is solved satisfying the current condition by setting the tangential component of $\mathbf{T}$ equal to zero on the interface of the conducting and nonconducting domains. In this situation the tangential component of $\mathbf{T}_0$ will satisfy the total current condition through the respective cross section of the conductor.

The properties of the function $\mathbf{T}_0$ are

$$\begin{aligned} curl\mathbf{T}_0 = \mathbf{0}, \quad \text{in } \Omega_n, \\ -\int_{\Gamma_E^i} curl\mathbf{T}_0 \cdot \mathbf{n}\, d\Gamma = \int_{\Gamma_E^0} curl\mathbf{T}_0 \cdot \mathbf{n}\, d\Gamma = i^i, \\ \mathbf{T}_0 \times \mathbf{n} \text{ is continous on } \Gamma_{cn}. \end{aligned} \tag{4.5}$$

There are several options for the selection of this function, the most convenient one in the general shape case is to assume current filaments in the conducting domain, between the two electrodes of each of the inductors carrying the prescribed current i^i. $\mathbf{T}_0$ in Ω_n is chosen to be the Biot-Savart field $\mathbf{H_s}$ due to these current filaments and is obtained as the solution of the following current flow problem in the conducting domain Ω_c:

$$\begin{aligned} curl\,(\rho curl\mathbf{T}_0) = \mathbf{0}, \quad \text{in } \Omega_c \\ \mathbf{T}_0 \times \mathbf{n} = \mathbf{H}_s \times \mathbf{n} \quad \text{on } \Gamma_{cn}, \\ \rho curl\mathbf{T}_0 \times \mathbf{n} = \mathbf{0} \text{ on } \Gamma_E^i, \Gamma_E^0. \end{aligned} \tag{4.6}$$

In case of simple inductor shapes, e.g. cylindrical or racetrack shapes, an economical choice of a single component $\mathbf{T}_0$ can be used to represent a uniform current density

distribution.

In the next step, the boundary value skin effect problem for $\mathbf{T}$ and Φ with the given function $\mathbf{T}_0$ is obtained, which consists of the differential equations (2.41), (2.42), (2.43) and the boundary conditions:

$$\rho curl\mathbf{T} \times \mathbf{n} = \mathbf{0}, \;\; \mu\left(\mathbf{T} - grad\Phi\right) \cdot \mathbf{n} = -\mu\mathbf{T}_0 \cdot \mathbf{n} \text{ on } \Gamma_E^i \text{ and on } \Gamma_E^0, \tag{4.7}$$

$$\mu\frac{\partial\Phi}{\partial n} = \mu\mathbf{T}_0 \cdot \mathbf{n} \text{ on } \Gamma_B, \tag{4.8}$$

$$\mathbf{T} \times \mathbf{n} = \mathbf{0}, \;\; \Phi \text{ and } \mu\left(\mathbf{T}_0 - grad\Phi\right) \cdot \mathbf{n} \text{ are continuous on } \Gamma_{cn} \tag{4.9}$$

4.3. Galerkin equations

Galerkin's method is applied to the above boundary value problem by approximating the potentials as

$$\begin{aligned} \mathbf{T} \approx \mathbf{T}_h &= \sum_{k\in E} T_k\mathbf{N}_k, \\ \Phi \approx \Phi_h &= \sum_{k\in N} \Phi_k N_k. \end{aligned} \tag{4.10}$$

Since all the Dirichlet boundary conditions for both $\mathbf{T}$ and Φ are homogenous, therefore no $\mathbf{T}_D$ and Φ_D functions are required. The given current condition is satisfied through the tangential components of $\mathbf{T}$ and $\mathbf{T}_0$ on conducting and non-conducting materials interface Γ_{cn} [42]. The resulting equations are

$$\begin{aligned} \int_{\Omega_c} curl\mathbf{N}_k \cdot \rho curl\mathbf{T}_h \, d\Omega + \frac{\partial}{\partial t}\left[\int_{\Omega_c} \mathbf{N}_k \cdot \mu\mathbf{T}_h \, d\Omega - \int_{\Omega_c} \mathbf{N}_k \cdot \mu grad\,\Phi_h \, d\Omega\right] \\ = -\int_{\Omega_c} curl\mathbf{N}_k \cdot \rho curl\mathbf{T}_0 \, d\Omega - \int_{\Omega_c} \mathbf{N}_k \cdot \frac{\partial}{\partial t}\left(\mu\mathbf{T}_0\right) \, d\Omega \end{aligned} \tag{4.11}$$

$$\begin{aligned} \frac{\partial}{\partial t}\left[-\int_{\Omega_c} gradN_k \cdot \mu\mathbf{T}_h \, d\Omega + \int_{\Omega} gradN_k \cdot \mu grad\,\Phi_h \, d\Omega\right] \\ = \int_{\Omega} gradN_k \cdot \frac{\partial}{\partial t}\left(\mu\mathbf{T}_0\right) \, d\Omega, \end{aligned} \tag{4.12}$$

Chapter 5

$\mathbf{T}, \Phi - \Phi$ Formulation of Skin Effect Problems with Voltage Excitation

In the $\mathbf{T}, \Phi - \Phi$ formulation, the prescribed voltage needs to be coupled with the potential functions. Here, the detailed approach to derive this formulation is shown considering the boundary value problem for multiply connected eddy current domain and external circuits with given voltages.

A multiply connected problem domain as shown in Fig. 5.1 is used to establish the relation between the potential functions and the electric global quantities. The current vector potential $\widetilde{\mathbf{T}}$ is introduced in the conducting region and the reduced magnetic scalar potential Φ in the whole problem domain. Additionally, a current vector potential or so called source field function $\mathbf{t}_0^i$ is used to take into account the unknown currents i^i associated with the electromotive force sources with given voltages and the multiply connected conducting domain [43, 44]. The curl of each of these functions is zero in the eddy current free domain, while it is non zero in the eddy current domain.

The potentials are introduced as:

$$\mathbf{H} = \mathbf{T} - grad\Phi = \sum_{i=1}^{n} i^i \mathbf{t}_0^i + \widetilde{\mathbf{T}} - grad\Phi \text{ in } \Omega, \tag{5.1}$$

and the current density field is given by

$$\mathbf{J} = \sum_{i=1}^{n} i^i curl\mathbf{t}_0^i + curl\widetilde{\mathbf{T}} \text{ in } \Omega_c \tag{5.2}$$

such that

$$\int_{\Gamma_i} curl\mathbf{t}_0^i = \oint_{\partial\Gamma_i} \mathbf{t}_0^i \cdot d\mathbf{l} = 1, \tag{5.3}$$

where Γ_i is any cross-section of the i^{th} inductor through which the net current i^i is flowing. The unit source field function can be obtained by assuming current filaments

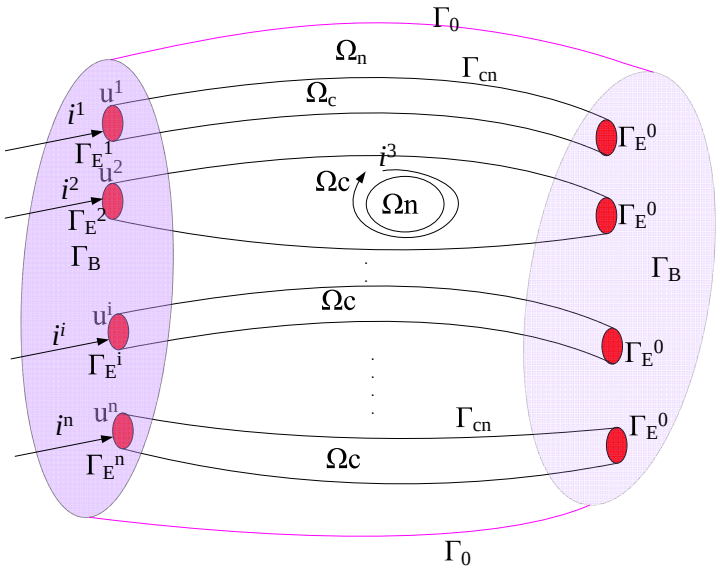

Figure 5.1 Bounded problem domain showing conductors with holes

of unit currents through the electrodes and also around the holes. These functions are represented with edge basis functions. The use of edge basis functions for the expansion of these functions guarantee the tangential continuity. The scalar potential function Φ is continuous in the whole problem domain.

5.1. Weak global constraint for the $\mathbf{T}, \Phi - \Phi$ formulation

The circuit relation in terms of potential functions is shown here for a single inductor. Consider an isolated portion of a thick conductor, as shown in Fig.5.2, with a voltage u applied across its two electrodes Γ_{E1} with scalar potential,v of value v_1 and Γ_{E2} with scalar potential value v_2 resulting in a current i flowing through it. The voltage in terms of the scalar potential values at the two terminals is $u = v_1 - v_2$.
Let us first assume that the current through the conductor is 1 A resulting in a current

density distribution of $\mathbf{J}_0(\mathbf{r})$. One such particular current density solution is obtainable by solving a current flow problem for unit current supplied through the electrodes [45]. Let the vector identity, $div(v\mathbf{J_0}) = \mathbf{J_0}{\cdot}gradv{+}vdiv\mathbf{J_0}$, be integrated over the conducting domain. Since $div\mathbf{J_0} = 0$;

$$\int_{\Omega_c} div(v\mathbf{J_0})\, d\Omega = \int_{\Omega_c} \mathbf{J_0} \cdot gradv\, d\Omega,$$
$$\int_{\Omega_c} \mathbf{J_0} \cdot gradv\, d\Omega = \oint_{\partial\Omega_c} v\mathbf{J_0} \cdot \mathbf{n}\, d\Gamma \tag{5.4}$$

the divergence theorem has been used to obtain the surface integral. Since $\mathbf{J_0} \cdot \mathbf{n} = 0$ on the conductor surface except on Γ_E,

$$\int_{\Omega_c} \mathbf{J_0} \cdot gradv\, d\Omega = \int_{\Gamma_{E1}} v_1\mathbf{J_0} \cdot \mathbf{n}\, d\Gamma + \int_{\Gamma_{E2}} v_2\mathbf{J_0} \cdot \mathbf{n}\, d\Gamma$$
$$= -v_1 + v_2 = -u_0 \tag{5.5}$$

The negative sign of the scalar potential v_1 is due to the fact that the assumed current density field and the unit normal vector at Γ_{E1} are in opposite direction whereas at Γ_{E2} the two are in the same direction as shown in Fig. 5.2. In general, the electric field intensity can be written in terms of the magnetic vector potential and the gradient of the electric scalar potential, as in (2.17), so the voltage across the two terminals is

$$u_0 = \int_{\Omega_c} \mathbf{J_0} \cdot \mathbf{E}\, d\Omega + \int_{\Omega_c} \mathbf{J_0} \cdot \frac{\partial \mathbf{A}}{\partial t}\, d\Omega. \tag{5.6}$$

The second integral on the right hand side can be written by using the vector identity, $div(\mathbf{A} \times \mathbf{t_0}) = \mathbf{t_0} \cdot curl\mathbf{A} - \mathbf{A} \cdot curl\mathbf{t}_0$, and writing $\mathbf{J_0}$ as $curl\mathbf{t_0}$:

$$\int_{\Omega_c} \mathbf{J}_0 \cdot \frac{\partial \mathbf{A}}{\partial t}\, d\Omega = \int_{\Omega_c} \mathbf{t}_0 \cdot \frac{\partial (curl\mathbf{A})}{\partial t}\, d\Omega - \frac{\partial}{\partial t} \int_{\partial\Omega_c} (\mathbf{A} \times \mathbf{t}_0) \cdot \mathbf{n}\, d\Gamma. \tag{5.7}$$

Let the support of the function $\mathbf{t}_0$, Ω_0 be selected such that it contains the conducting domain, Ω_c entirely, so that a closed path around the conductor runs within Ω_0. Let the choice of the function $\mathbf{t}_0$ be made such that its tangential component vanishes on $\partial\Omega_0$ and it satisfies $\mathbf{J_0} = curl\mathbf{t_0}$ within Ω_0. In this way, by expanding the surface integral to the far boundary Γ_0, it vanishes.

$$u_0 = \int_{\Omega_c} \mathbf{J_0} \cdot \mathbf{E}\, d\Omega + \int_{\Omega_0} \mathbf{t_0} \cdot \frac{\partial \mathbf{B}}{\partial t}\, d\Omega. \tag{5.8}$$

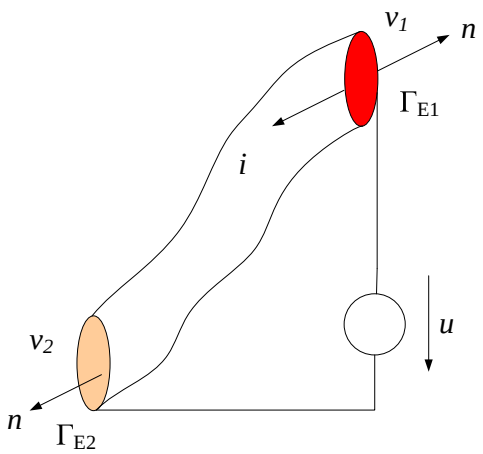

Figure 5.2 Massive conductor with voltage source.

The above relation can be generalized for a conducting domain with multiple electrodes and perforated conducting domain. For each of the external circuits, the above relation will hold, so

$$u^i = \int_{\Omega_c} \mathbf{J}_0^i \cdot \mathbf{E}\, d\Omega + \int_{\Omega_0} \mathbf{t}_0^i \cdot \frac{\partial \mathbf{B}}{\partial t}\, d\Omega, \tag{5.9}$$

where superscript i stands for the i^{th} source.

5.2. Boundary value problem

Faraday's law (2.3) and the divergence free property of the magnetic flux density, **B** (2.4) constitute the differential equations for the potentials.

$$curl\left(\rho\sum_{i=1}^{n} i^i curl\mathbf{t}_0^i\right) + curl\left(\rho curl\widetilde{\mathbf{T}}\right)$$
$$+\frac{\partial}{\partial t}\left(\mu\sum_{i=1}^{n} i^i\mathbf{t}_0^i + \mu\widetilde{\mathbf{T}} - \mu grad\Phi\right) = 0 \text{ in } \Omega_c, \tag{5.10}$$

$$\frac{\partial}{\partial t} div\left(\mu\sum_{i=1}^{n} i^i\mathbf{t}_0^i + \mu\widetilde{\mathbf{T}} - \mu grad\Phi\right) = 0 \text{ in } \Omega_c, \tag{5.11}$$

$$\frac{\partial}{\partial t} div\left(\mu\sum_{i=1}^{n} i^i\mathbf{t}_0^i - \mu grad\Phi\right) = 0 \text{ in } \Omega_n. \tag{5.12}$$

whereas ρ is the resistivity and μ the permeability.

Boundary and interface conditions of the problem obtained in terms of potential functions, using (2.5) and (2.8), are

$$\rho curl\mathbf{T}\times\mathbf{n} = \mathbf{0},\ \ \mu\left(\sum_{i=1}^{n} i^i\mathbf{t}_0^i + \widetilde{\mathbf{T}} - grad\Phi\right) \text{ on } \Gamma_E^i \text{ and } \Gamma_E^0\ , \tag{5.13}$$

$$\mu\left(\sum_{i=1}^{n} i^i\mathbf{t}_0^i - grad\Phi\right)\cdot\mathbf{n} = 0 \text{ on } \Gamma_B, \tag{5.14}$$

$$\mathbf{n}_c\times\widetilde{\mathbf{T}} = \mathbf{0},\ \mathbf{n}_c\times\mathbf{t}_0^i = \mathbf{n}_n\times\mathbf{t}_0^i,\quad \mathbf{n_c}\cdot\left(\mu\sum_{i=1}^{n} i^i\mathbf{t}_0^i + \mu\widetilde{\mathbf{T}} - \mu grad\Phi\right)$$
$$+\mathbf{n_n}\cdot\left(\mu\sum_{i=1}^{n} i^i\mathbf{t}_0^i - \mu grad\Phi\right) = 0 \quad \text{on } \Gamma_{cn}, \tag{5.15}$$

5.3. Galerkin equations

The potentials are approximated as

$$\mathbf{T} \approx \mathbf{T}_h = \sum_{i=1}^{n} i^i\mathbf{t}_0^i + \sum_{k=0}^{n_1} T_k\mathbf{N}_k,$$
$$\Phi \approx \Phi_h = \sum_{k=0}^{n_2} \Phi_k N_k \tag{5.16}$$

where n_1 is the number of edges in the conducting domain and n_2 the number of nodes in the whole domain..

The operator equation (5.10) is weighted with the functions $\mathbf{N}_k$ and also with the functions $\mathbf{t}_0^i$. The equations (5.11) and (5.12) are weighted with N_k functions. The resulting Galerkin equations are:

$$\int_{\Omega_c} curl\mathbf{N}_k \cdot \rho curl\mathbf{T}_h \, d\Omega + \frac{\partial}{\partial t}\left[\int_{\Omega_c} \mathbf{N}_k \cdot \mu\mathbf{T}_h \, d\Omega - \int_{\Omega_c} \mathbf{N}_k \cdot \mu grad\, \Phi_h \, d\Omega\right] = 0 \quad (5.17)$$

$$\int_{\Omega_c} curl\mathbf{t}_0^i \cdot \rho curl\mathbf{T}_h \, d\Omega$$
$$+\frac{\partial}{\partial t}\left[\int_{\Omega_c} \mathbf{t}_0^i \cdot \mu\mathbf{T}_h \, d\Omega - \int_{\Omega_c} \mathbf{t}_0^i \cdot \mu grad\, \Phi_h \, d\Omega\right] = u^i \quad i = 1, 2, \cdots, n \,, \quad (5.18)$$

$$\frac{\partial}{\partial t}\left[-\int_{\Omega} gradN_k \cdot \mu\mathbf{T}_h \, d\Omega + \int_{\Omega} gradN_k \cdot \mu grad\, \Phi_h \, d\Omega\right] = 0 \quad (5.19)$$

u^i is the given voltage of the i^{th} source, and is zero for the holes.

Chapter 6

$\mathbf{A}, v - \mathbf{A}$ Formulation of Skin Effect Problems with Current Excitation

In this chapter, the introduction of a new nodal basis function which is the sum of the nodal basis functions corresponding to the nodes on each of the electrodes with given current condition is presented. In order to extend the $\mathbf{A}, v - \mathbf{A}$ formulation to take into account the current sources, the unspecified Dirichlet boundary conditions for the scalar potential demand a special treatment. The treatment of the incompletely specified boundary condition for the scalar potential at the electrodes is presented and the system of Galerkin equations is obtained.
It is also shown that the prescribed current condition is a weak global constraint in this formulation and

6.1. Boundary value problem

The problem of Fig. 3.1 is now considered with the condition of given currents i^n instead of voltages u^n . The Dirichlet boundary condition for the scalar potential of (3.10) is not completely specified because of the unknown voltages of the sources.

The boundary value problem comprises the differential equations (2.19), (2.20), (2.21) in terms of potential functions and the boundary conditions

$$\mathbf{n} \times \mathbf{A} = \mathbf{0}, \quad \text{and } v = \textit{unknown constant } v_0^i \quad \text{on each of the } \Gamma_E^i, \tag{6.1}$$

$$\mathbf{n} \times \mathbf{A} = \mathbf{0} \text{ and } v = 0 \quad \text{on each of the } \Gamma_E^0, \tag{6.2}$$

$$\mathbf{n} \times \mathbf{A} = 0 \quad \text{on } \Gamma_B \tag{6.3}$$

$$\nu curl \mathbf{A} \times \mathbf{n} = \mathbf{0} \text{ on } \quad \Gamma_{H_n}, \tag{6.4}$$

$$\nu curl\mathbf{A} \times \mathbf{n} = \mathbf{0} \text{ and}$$
$$\mathbf{n} \cdot -\sigma \frac{\partial}{\partial t} (\mathbf{A} + grad v) = 0 \text{ on } \Gamma_{H_c} \tag{6.5}$$

The prescribed current in terms of the scalar potential in (6.1) is the only essential non homogeneous boundary condition to be satisfied on each of the source electrodes Γ_E^i.

6.2. Galerkin equations

The potential functions are approximated as

$$\mathbf{A} \approx \mathbf{A}_h = \sum_{k=1}^{n_1} A_k \mathbf{N}_k, v \approx v_h = \sum_{i=1}^{n} v_D^i + \sum_{k=1}^{n_2} v_k N_k, \tag{6.6}$$

$$v_D^i = \sum_{nodes_j \in \Gamma_E^i} v_j^i N_j^i, \tag{6.7}$$

where n_1 is the number of edges in Ω excluding those on Γ_E^i, the far boundary, Γ_0 and n_2 is the number of nodes in Ω_c excluding those on Γ_E^i. v_D^i is the modified scalar potential function corresponding to the electrode Γ_E^i of the i^{th} source, through which the total current is given and n is the number of inductors or the electrodes of the sources in the problem with prescribed currents. Since the electrodes are equipotential surfaces [46],

$$v_D^i = v_0^i \sum_{nodes_j \in \Gamma_E^i} N_j^i, \tag{6.8}$$

$$\sum_{nodes_j \in \Gamma_E^i} N_j^i = N_{\Gamma_E^i}, \tag{6.9}$$

$$v_D^i = v_0^i N_{\Gamma_E^i}, \tag{6.10}$$

The function $N_{\Gamma_E^i}$ is the new basis function that is further used as weighting function to complete the formulation for the given current condition. The function $N_{\Gamma_E^i}$ has its support limited to the elements which include at least one of the nodes on Γ_E^i, that is only to a single layer adjacent to Γ_E^i. As an example, an inductor is shown in Fig. 6.1 in which the support of this new function is shown. The function $N_{\Gamma_E^i}$ is equal to 1 on Γ_E^i, i.e. it corresponds to the source of a unit modified potential on Γ_E^i.

Two sets of Galerkin finite element equations (3.16) and (3.17) describe the $\mathbf{A}, v - \mathbf{A}$ formulation for problems with given voltages. Another set is now needed to complete the formulation, due to addition of the n unknown voltages.
Since the boundary condition on the electrode with prescribed current condition, Γ_E^i

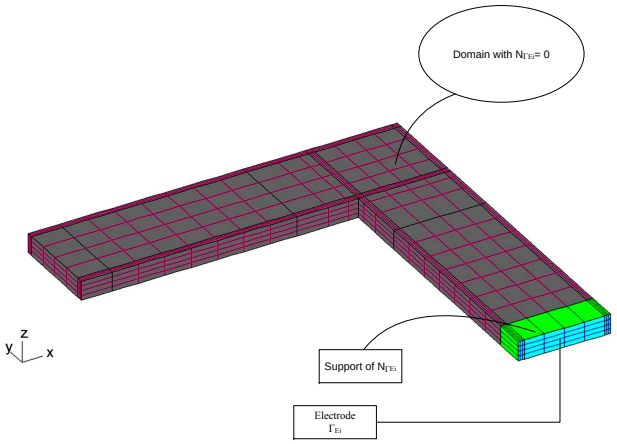

Figure 6.1 Support of $N_{\Gamma_E^i}$ in a massive rectangular Conductor/inductor.

introduces an additional unknown v_0^i, the unknown constant value of the scalar potential on Γ_E^i, an additional equation for each electrode is required to complete the equation system.

Furthermore, the surface integral relation

$$\int_{\Gamma_E^i} \sigma(\frac{\partial \mathbf{A}}{\partial t} + grad\frac{\partial v}{\partial t}) \cdot \mathbf{n}\, d\Gamma = i^i, \tag{6.11}$$

is to be satisfied for each of the electrodes Γ_E^i through which the total current is prescribed.

The function $N_{\Gamma_E^i}$ is used as the weighting function along with the potentials approximations (6.6) and (6.7) for $div\mathbf{J} = 0$ to write the required additional equation as

$$\begin{aligned} &\int_{\Omega_c} N_{\Gamma_E^i}[-div\sigma\frac{\partial}{\partial t}(\mathbf{A}_h + gradv_h)]\, d\Omega \\ &+ \int_{\Gamma_{cn}} N_{\Gamma_E^i}[\sigma\frac{\partial}{\partial t}\mathbf{n} \cdot (\mathbf{A}_h + gradv_h)]\, d\Gamma = 0. \end{aligned} \tag{6.12}$$

By using the vector identity, $f\, div\mathbf{F} = div(f\mathbf{F}) - \mathbf{F} \cdot grad\, f$, with $\mathbf{F}$ and f any vector

and any scalar function respectively, and Gauss law it becomes

$$\begin{aligned}
&\int_{\Omega_c} gradN_{\Gamma_E^i} \cdot \sigma \frac{\partial}{\partial t}(\mathbf{A}_h + gradv_n)]\, d\Omega \\
&- \oint_{\Gamma_{cn}+\Gamma_E^i+\Gamma_E^0} N_{\Gamma_E^i}[\sigma \frac{\partial}{\partial t}\mathbf{n} \cdot (\mathbf{A}_h + gradv_h)]\, d\Gamma \\
&+ \int_{\Gamma_{cn}} N_{\Gamma_E^i}[\sigma \frac{\partial}{\partial t}\mathbf{n} \cdot (\mathbf{A}_h + gradv_h)]\, d\Gamma = 0. \qquad (6.13)
\end{aligned}$$

The surface integrals on Γ_{cn} cancel out, on Γ_E^0 it is zero because $N_{\Gamma_E^i}$ is zero there, and, since $N_{\Gamma_E^i}$ is 1 on Γ_E^i,

$$\begin{aligned}
&\int_{\Omega_c} gradN_{\Gamma_E^i}.\sigma \frac{\partial}{\partial t}(\mathbf{A}_\mathbf{n} + gradv_n)]\, d\Omega \\
&- \int_{\Gamma_E^i} [\sigma \frac{\partial}{\partial t}\mathbf{n} \cdot (\mathbf{A}_\mathbf{n} + gradv_n)]\, d\Gamma = 0. \qquad (6.14)
\end{aligned}$$

Using (6.11), the additional set of equations is written as

$$\int_{\Omega_c} gradN_{\Gamma_E^i}.\sigma \frac{\partial}{\partial t}(\mathbf{A}_h + gradv_h)\, d\Omega = i^i, \quad i = 1, 2, ..., n\ . \qquad (6.15)$$

Therefore the complete set of Galerkin equations for the $\mathbf{A}, v - \mathbf{A}$ formulation of skin effect problems with current excitation consists of (3.16), (3.17) and (6.15). The system of equations is singular but symmetric with $n_1 + n2 + n$ degrees of freedom and the same number of equations.

6.3. Weak global constraint for the $\mathbf{A}, v - \mathbf{A}$ formulation

The total current is the flux type quantity which is only weakly conserved in the magnetic vector potential formulation [47]. Therefore, the total current flowing in a conductor is only expressed in a weak sense. It is coupled with the field quantities through Ampere law which is itself expressed in the weak form. The current i^i through any cross section of the inductor is defined by (6.11). It becomes apparent by using $N_{\Gamma_E^i}$ as the weighting function in the weak formulation of $div\mathbf{J} = 0$. The same approach is adopted in the last section to obtain Galerkin equations.

Chapter 7

Transient Skin Effect Problems

The motivation of this chapter is to present the extension of the new feature of the $\mathbf{A}, v-\mathbf{A}$ formulation to transient skin effect problems as well. The techniques already developed for the linear and nonlinear transient problems at the Institute for Fundamentals and Theory in Electrical Engineering (IGTE) were used for this work.
The formulations presented in the preceding chapters result in a system of ordinary differential equations which has to be solved, in the general case of transient problems, in the time domain [48]. The general form of these equations showing the time dependence explicitly is

$$\mathbf{S}(t)\mathbf{x}(t) + \mathbf{M}\frac{d\mathbf{x}(t)}{dt} = \mathbf{f}(t), \tag{7.1}$$

for the $\mathbf{A}, v-\mathbf{A}$ formulation and

$$\mathbf{S}\mathbf{x}(t) + \frac{d}{dt}\left(\mathbf{M}(t)\mathbf{x}(t)\right) = \mathbf{f}(t), \tag{7.2}$$

for the $\mathbf{T}, \Phi-\Phi$ formulation.

The vector $\mathbf{x}(t)$ is the vector of unknown potentials and $\mathbf{f}(t)$ correspond to the given forcing term. The system matrices $\mathbf{S}(t)$ and $\mathbf{M}(t)$ are, in case of nonlinear problems, time dependent because of their dependence on the solution vector $\mathbf{x}(t)$ depending on the potential formulations employed. The stiffness matrix $\mathbf{S}(t)$ is a function of ν in the $\mathbf{A}, v-\mathbf{A}$ formulation which depends on the potentials. In contrast, it is a function of ρ in the $\mathbf{T}, \Phi-\Phi$ formulation which does not depend on the solution vector. On the other hand, the mass matrix $\mathbf{M}(t)$ is a function of μ in the $\mathbf{T}, \Phi-\Phi$ formulation which depends on the potentials. In contrast, it is a function of σ in the $\mathbf{A}, v-\mathbf{A}$ formulation which does not depend on the solution vector.

The above system of equations is to be solved by time stepping method in general and in special periodic case the stepping through several periods can be avoided.

7.1. General excitation

If the excitations are non-periodic the only option to solve the resultant system of Galerkin equation is to use the time stepping technique, the so called brute force method. This technique is also necessary if the transient solution is required. The time stepping technique is applicable to linear as well as nonlinear problems. The unknowns of the equations are sought at discrete time instants $t_k(1, 2, \cdots, N)$

$$t_k = \sum_{i=1}^{k} \Delta t_i, (k = 1, 2, \cdots). \tag{7.3}$$

Δt_i is the length of the i^{th} time step.

Let the time interval be chosen so small that the variation of the time dependent quantities $\mathbf{x}(t)$ and $\mathbf{f}(t)$ can be assumed to be linear. In Fig. 7.1, the linear interpolation of $x(t)$, which is a component of $\mathbf{x}(t)$, is shown between two consecutive time instants. The function $\mathbf{x}(t)$ is interpolated for $t \in [t_{k-1}, t_k]$ as

$$\mathbf{x}(\tau) = \mathbf{x}_{k-1} + \frac{\tau}{\Delta t} \left(\mathbf{x}_k - \mathbf{x}_{k-1} \right), \tag{7.4}$$

where

$$\tau = t - t_{k-1} \tag{7.5}$$

whereas $\dot{\mathbf{x}}$ is approximated between the two time instants as

$$\dot{\mathbf{x}} = \frac{1}{\Delta t} \left(\mathbf{x}_k - \mathbf{x}_{k-1} \right). \tag{7.6}$$

Setting $\mathbf{x}$ and $\dot{\mathbf{x}}$, from (7.4) and (7.6) respectively, in (7.1) or (7.2) and weighting it with an arbitrary weighting function w results in the system of equations

$$\int_0^{\Delta t} \left(\mathbf{S}\mathbf{x}(\tau) + \mathbf{M}\dot{\mathbf{x}}(\tau) - \mathbf{f}(\tau) \right) w \, d\tau = \mathbf{0}, \tag{7.7}$$

where w is some weighting function. This results in each time dependent quantity $f(t)$ not differentiated with respect to time being replaced by

$$f(t) = \Theta f_k + (1 - \Theta) f_{k-1}, \tag{7.8}$$

and the time derivative by

$$\dot{f} = \frac{1}{\Delta t}(f_k - f_{k-1}), \tag{7.9}$$

where Θ is a factor given by

$$\Theta = \frac{1}{\Delta t} \frac{\int_0^{\Delta t} w\tau \, d\tau}{\int_0^{\Delta t} w \, d\tau}, \qquad \text{with } \Theta \in [0, 1]. \tag{7.10}$$

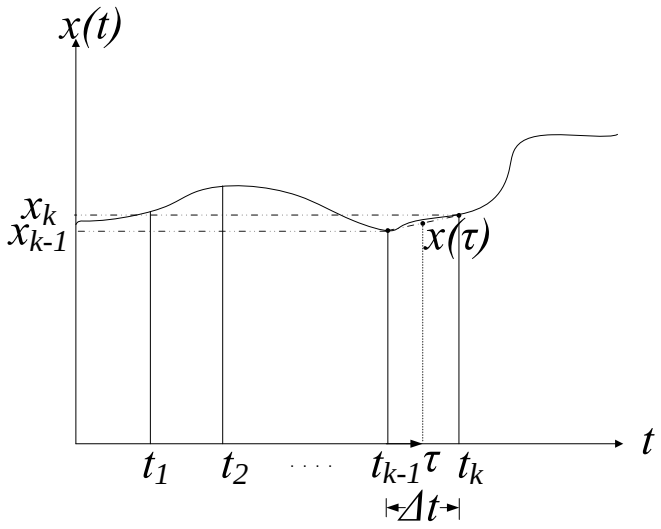

Figure 7.1 Linear interpolation of a time function $x(t)$.

Some special values of Θ results in the following specific methods [49]:

$\Theta = 0$: forward Euler method,
$\Theta = 1$: backward Euler method,
$\Theta = 1/2$: Crank-Nicholson method,
$\Theta = 2/3$: Galerkin method.

Using (7.8) and (7.9), (7.1) can be written as

$$\left(\Theta\mathbf{S}_k + \frac{1}{\Delta t}\mathbf{M}\right)\mathbf{x}_k + \left((1-\Theta)\,\mathbf{S}_{k-1} - \frac{1}{\Delta t}\mathbf{M}\right)\mathbf{x}_{k-1} = \Theta\mathbf{f}_k + (1-\Theta)\,\mathbf{f}_{k-1}. \quad (7.11)$$

The equation (7.2) becomes

$$\left(\Theta\mathbf{S}+\frac{1}{\Delta t}\mathbf{M}_k\right)\mathbf{x}_k+\left((1-\Theta)\,\mathbf{S}-\frac{1}{\Delta t}\mathbf{M}_k\right)\mathbf{x}_{k-1}=\Theta\mathbf{f}_k+(1-\Theta)\,\mathbf{f}_{k-1}. \tag{7.12}$$

The solution of the systems of equations (7.11) and 7.12 is straightforward, i.e. starting with an initial solution $\mathbf{x}_0$, the unknown vector $\mathbf{x}_1$ is obtained. Knowing $\mathbf{x}_1$, $\mathbf{x}_2$ can be obtained. In general, $\mathbf{x}_k$ is obtained with $\mathbf{x}_{k-1}$ given. The choice of the initial solution $\mathbf{x}_0=\mathbf{0}$ is always available to start the time stepping procedure. So with the time stepping method, the system of equations (7.1) and (7.2) is reduced to systems of algebraic equations in the time domain analysis [50] [51].

The time discretized equation system for both potential formulations can be written as

$$\bar{\mathbf{S}}_k\mathbf{x}_k+\bar{\mathbf{M}}_{k-1}\mathbf{x}_{k-1}=\bar{\mathbf{f}}_{k,k-1},\qquad \text{for } k=1,2,\cdots,N, \tag{7.13}$$

with the system matrices

$$\bar{\mathbf{S}}_k=\Theta\mathbf{S}_k+\frac{1}{\Delta t}\mathbf{M}_k, \tag{7.14}$$

$$\bar{\mathbf{M}}_{k-1}=-\left((1-\Theta)\,\mathbf{S}_{k-1}+\frac{1}{\Delta t}\mathbf{M}_{k-1}\right), \tag{7.15}$$

and the forcing function term

$$\bar{\mathbf{f}}_{k,k-1}=\Theta\mathbf{b}_k+(1-\Theta)\,\mathbf{f}_{k-1}, \tag{7.16}$$

where $\mathbf{S}_k$ and $\mathbf{M}_k$ are as given in (7.1) and (7.2). The index k stands for the k^{th} time step and also shows the nonlinear dependence of the system matrices on the ferromagnetic material properties. If n is the number of degrees of freedom (DoF) in the finite element mesh, a nonlinear equation system with $n.N$ unknowns has to be solved. Starting with an initial solution $\mathbf{x}_0$, in every time step k the equation system (7.13) is to be solved.

7.2. Time periodic excitation

For the special time periodic case and an equal interval time step, Δt is given as

$$\Delta t=\frac{T}{N}, \tag{7.17}$$

where T is the time period and N the number of time steps within one time period. After the transients decay, the steady state solution is periodic with the same period T

as that of the harmonic excitation [52]. The following periodicity condition holds for the potentials obtained with the computation:

$$\mathbf{x}(t) = \mathbf{x}(t + T). \tag{7.18}$$

The above relation is true for every component of the unknown vector $\mathbf{x}$. A typical periodically varying component of $\mathbf{x}$ is shown in Fig. 7.2. Let the periodicity condition (7.18) be achieved after a minimum time t_s then

$$t_s = pT, \tag{7.19}$$

where p is the number of periods to be computed to obtain the steady state solution. The total number of time steps to obtain the steady state solution is then $n = 1, 2, \cdots, N.p$ where N is the number of time steps within one period. If homogeneous initial conditions $\mathbf{x} = \mathbf{0}$ are given, it is necessary to compute over p periods until (7.18) is satisfied approximately. The transient skin effect problem with periodic

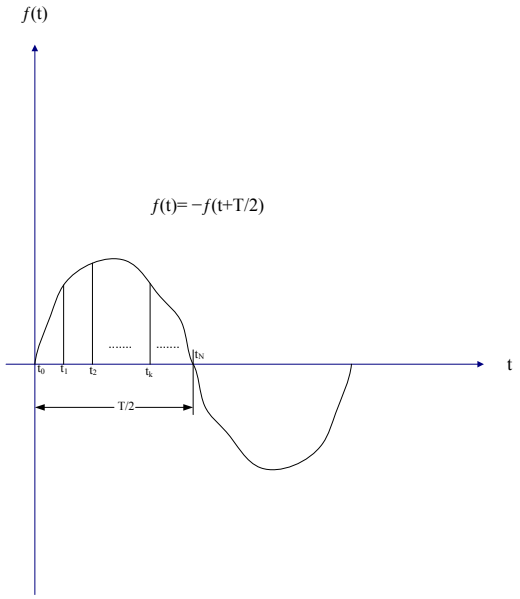

Figure 7.2 General time harmonic potential function $f(t)$ after steady state.

excitation can be efficiently solved in the time domain by stepping through only one period by enforcing the periodicity condition. In the frequency domain, the harmonic balance method can also be used to solve such problems efficiently. Both methods are

briefly described here. The current prescription condition, in the $\mathbf{A}, v-\mathbf{A}$ formulation, is implemented in the software environment (EleFAnT 3D) for the linear and nonlinear transient skin effect problems.

7.2.1. Linear case

Since the vector of the forcing function is time periodic with a period T there exists a periodic steady-steady state solution satisfying the periodicity condition $\mathbf{x}(0) = \mathbf{x}(T)$. N coupled linear equation systems are obtained as a result of the time discretization of (7.1) within one period with a constant time step $\Delta t = T/N$

$$\mathbf{A}\mathbf{x}_k + \mathbf{B}\mathbf{x}_{k-1} = \mathbf{f}_k \qquad \text{for } k = 1, 2, \cdots, N, \tag{7.20}$$

where $\mathbf{A}$ and $\mathbf{B}$ are linear combinations of the matrices $\mathbf{S}$ and $\mathbf{M}$, $\mathbf{f}_k$ is a linear combination of the known vectors $\mathbf{f}(k\Delta t)$ and $\mathbf{f}((k-1)\Delta t)$ and $\mathbf{x}_k = \mathbf{x}(k\Delta t)$ is the vector of unknowns at the k^{th} time step. To obtain the steady-state solution the periodicity condition, $\mathbf{x}_0 = \mathbf{x}_N$, is enforced. Block-diagonalization can be applied after arranging the solution $\mathbf{x}_k$ and right hand side vectors for N time instants within a period [53]. With the use of discrete Fourier transform $N/2$ linear systems are required to be solved. Time domain steady state solution is obtained by the inverse Fourier transformation.

Another option to solve the linear problem is the application of harmonic balance method in the frequency domain [54]. The differential equation (7.1) can be transformed into the frequency domain by writing

$$\mathbf{x}(t) = Re\{\mathbf{X}e^{j\omega t}\}, \quad f(t) = Re\{\mathbf{F}e^{j\omega t}\} \tag{7.21}$$

where ω is the angular frequency and j represents the imaginary unit. Using the above relation, (7.1) can be written in the complex form as:

$$(\mathbf{S} + j\omega\mathbf{M}) \cdot \mathbf{X} = \mathbf{F} \tag{7.22}$$

7.2.2. Nonlinear case

The case of the $\mathbf{A}, v-\mathbf{A}$ formulation is considered here. As in the nonlinear problem the relation between the magnetic field intensity, $\mathbf{H}$ and the flux density $\mathbf{B}$ is nonlinear, the matrix $\mathbf{S}$ in (7.1) and, hence, the matrices $\mathbf{A}$ and $\mathbf{B}$ in (7.20) depend on x_k, therefore the Fourier block-diagonalization presented in the previous section is not possible. In this case, the magnetic field intensity can be decomposed in linear and nonlinear parts as

$$\mathbf{H} = \nu_{FP}\mathbf{B} - \mathbf{M}_{FP} \tag{7.23}$$

where ν_{FP} is an appropriate reluctivity independent of $\mathbf{B}$ and $\mathbf{M}_{FP}$ is a field dependent magnetization-like quantity. Starting with an arbitrary $\mathbf{M}_{FP}$, it is updated at

each iteration step. The value of the so called fixed point reluctivity ν_{FP} is chosen for the better rate of convergence of the method [55].

The choice of a fixed value of ν_{FP} at every time step makes the matrices $\mathbf{A}$ and $\mathbf{B}$ unaltered for all values of k, so the block-diagonalization of the previous section becomes applicable at every nonlinear iteration step. In contrast, the right hand side becomes dependent on the problem variables, which can be easily managed with the use of iterative approach. It can be determined using the previous time step solution in (7.23).

The fixed point method [56] together with the harmonic balance method allows the linearization of the finite element Galerkin equations. The equations for each harmonic are decoupled in this way.

Using (7.23) in (7.1), $\mathbf{S}$ and $\mathbf{M}$ become independent of $\mathbf{x}$, but the right hand side $\mathbf{f}$ will depend on the unknowns:

$$\widetilde{\mathbf{S}}\,\mathbf{x}(t) + \widetilde{\mathbf{M}}\,\dot{\mathbf{x}}(t) = \widetilde{\mathbf{f}}(\mathbf{x}, t). \tag{7.24}$$

where $\widetilde{\mathbf{f}}(\mathbf{x}, t)$ contains the excitation and a term which corresponds to $\mathbf{M}_{FP}$ [54]. Because $\mathbf{M}_{FP}$ is a function of $\mathbf{B}$ therefore right hand side of (7.24) depends on $\mathbf{x}$. Solving (7.24) iteratively, the vector $\widetilde{\mathbf{f}}$ in an iteration step is determined from the solution $\mathbf{x}$ of the previous step using (7.23). Once $\widetilde{\mathbf{f}}$ is determined, the vector depends on time only. So (7.24) transforms into the same form as that of (7.1):

$$\widetilde{\mathbf{S}}\,\mathbf{x}(t) + \widetilde{\mathbf{M}}\,\dot{\mathbf{x}}(t) = \widetilde{\mathbf{g}}(t). \tag{7.25}$$

The vectors x and $\widetilde{g}$ are approximated as complex Fourier-series with N harmonics:

$$\begin{aligned} \mathbf{x}(t) &\cong Re\left\{\mathbf{X}_0 + \sum_{n=1}^{N} \mathbf{X}_n e^{jn\omega_0 t}\right\}, \\ \widetilde{\mathbf{g}}(t) &\cong Re\left\{\widetilde{\mathbf{G}}_0 + \sum_{n=1}^{N} \widetilde{\mathbf{G}}_n e^{jn\omega_0 t}\right\} \end{aligned} \tag{7.26}$$

where ω_0 is the angular frequency of the excitation. $\mathbf{X}_0$ and $\widetilde{\mathbf{G}}_0$ are the DC-components and $\mathbf{X}_n$ and $\widetilde{\mathbf{G}}_n$ are the complex amplitudes at frequency $n\omega_0$. The approximations of $\mathbf{x}$ and $\widetilde{\mathbf{g}}$ together with (7.25) lead to $N+1$ linear decoupled equation systems:

$$\widetilde{\mathbf{S}}\mathbf{X}_0 = \widetilde{\mathbf{G}}_0, \quad \left(\widetilde{\mathbf{S}} + jn\omega_0\widetilde{\mathbf{M}}\right)\cdot \mathbf{X}_n = \widetilde{\mathbf{G}}_n, \;\; n = 1, 2, \cdots, N. \tag{7.27}$$

The amplitudes are calculated from the time signals by the so called Discrete Fourier Transform (DFT):

$$\widetilde{\mathbf{G}}_0 = \frac{1}{\mathbf{M}} \sum_{k=0}^{M-1} \widetilde{\mathbf{g}}(k\Delta t), \quad \widetilde{\mathbf{G}}_n = \frac{2}{\mathbf{M}} \sum_{k=0}^{M-1} \widetilde{\mathbf{g}}(k\Delta t) e^{-j\frac{2\Pi/M}{n}k}, \;\; n = 1, 2, \cdots, M-1, \tag{7.28}$$

where M is the number of time values for $\widetilde{\mathbf{g}}$ and Δt is the time step.

Chapter 8

Applications and Results

The validation of the newly developed technique, the $\mathbf{A}, v - \mathbf{A}$ formulation with current prescription condition, is carried out by selecting some problems in the frequency domain, which are also solvable with the other techniques presented in *chapters 3 − 5*. Afterwards an industrial application is shown by presenting the analysis results of an induction machine problem. The extension of the method to the transient case is verified with its application to the steady state problem already solved in the frequency domain.

8.1. A multi turn reactor coil problem

A square (2400 mm) coil of copper ($\mu = \mu_0, \sigma = 5.7 \times 10^7$ S/m) rectangular conductor (300mm x 60mm) reactor arrangement consisting of twenty turns is studied. The gap between each turn is 20 mm while the distance of the first conductor above the symmetry plane is 150 mm.

A sinusoidal ($f = 50\,Hz$) current of 100,000 amperes is given through each of the electrodes on the xz plane, while electrodes on the other end are the reference electrodes with zero scalar potential on each of them.
Due to the time varying magnetic field, an electric field is induced in the coil conductor resulting in a typical skin effect problem. The problem has been analyzed both by the $\mathbf{A}, v - \mathbf{A}$ and the $\mathbf{T}, \Phi - \Phi$ formulation on the same grid. Forces acting on each of the turns of the winding are determined and also the inductance of the arrangement is computed.

8.1.1. Model of one eighth Problem

Only one eighth of the problem is sufficient to be modeled due to symmetry. The geometry of the problem is defined starting with an initial grid. The rectangular grid elements are so called macro elements which are further divided into finite elements by specifying the subdivisions. Material properties are also defined at macro element

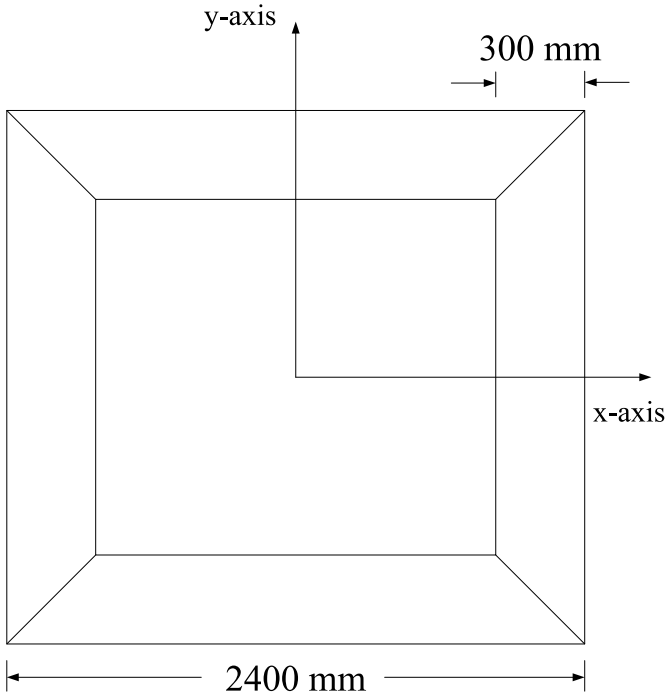

Figure 8.1 Top view of the coil and its dimensions

level. The model of this problem consists of 1078 macro elements, as shown in Fig. 8.2 with three symmetry planes passing through the origin and three far boundaries at distance of 10 meters from the problem origin. The model structure is subdivided into finite elements keeping in mind the problem symmetry and expected skin effect. A relatively finer mesh is used for the outer surfaces of the conductors. The finite element discretization resulting in 96,775 second order hexahedral elements is shown in Fig. 8.3.The same mesh is used for both the formulations.

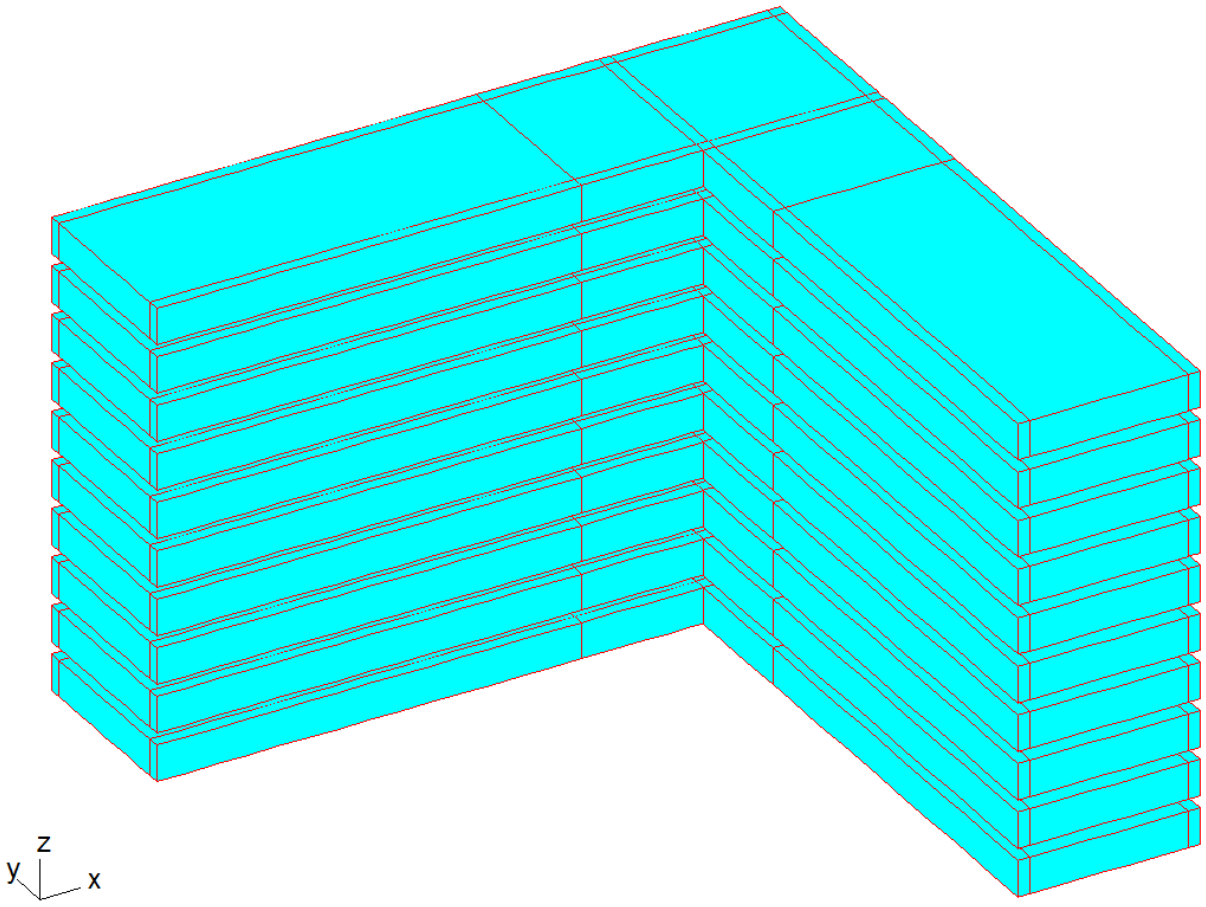

Figure 8.2 Macro element structure

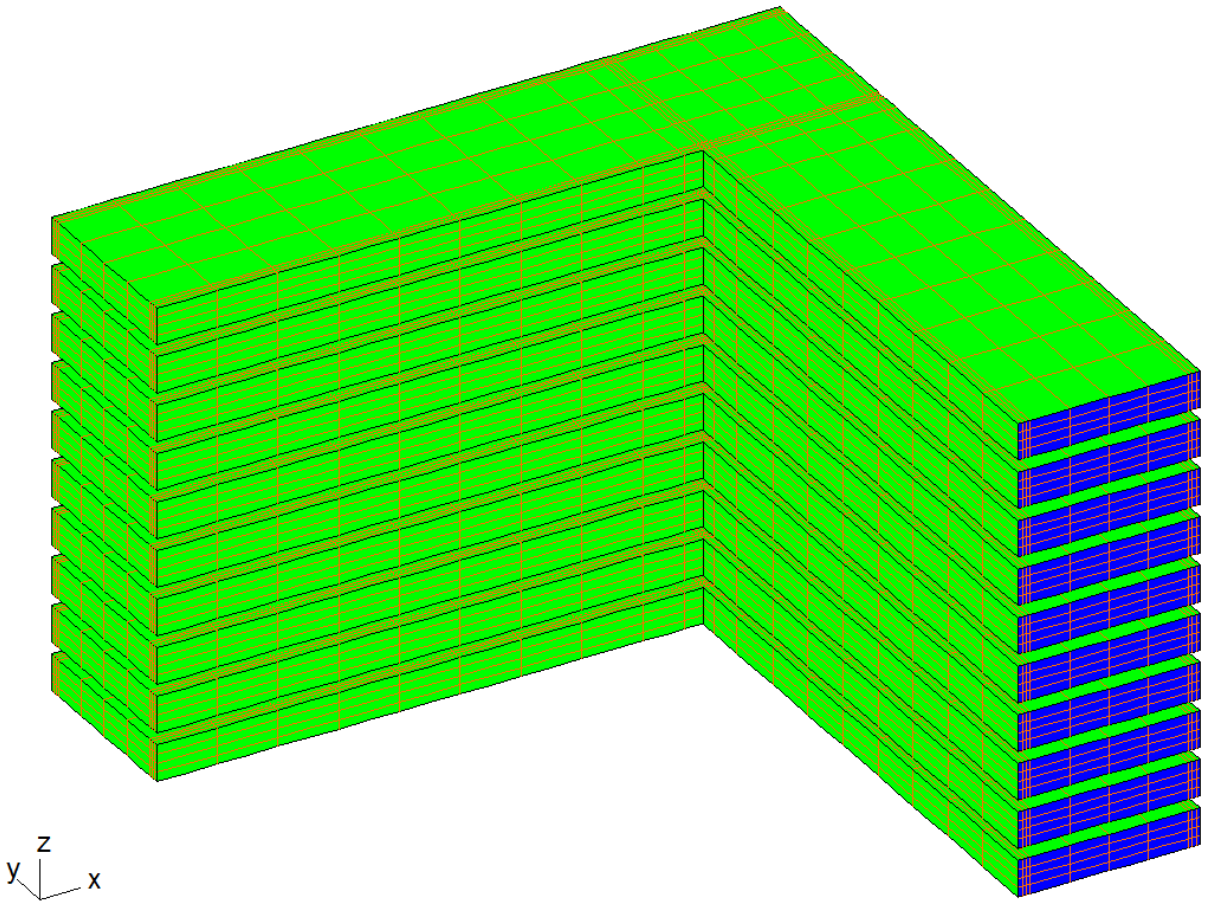

Figure 8.3 Finite element mesh.

8.1.2. Comparison of results

The resulting system of algebraic equations has been solved by the conjugate gradient (CG) technique. The current has been prescribed in the $\mathbf{A}, v-\mathbf{A}$ version by setting the scalar potential to an unknown constant value on each of the electrodes shown shaded in Fig. 8.3. In the $\mathbf{T}, \Phi - \Phi$ approach, $\mathbf{T}_0$ has been chosen as the Biot-Savart field of the filamentary current carrying conductors through the middle of each rectangular conductor in the air region, whereas a static current flow problem is first solved in the conducting domain. The current density obtained as solution of the static current flow problem along with the assumed current filaments is shown in Fig. 8.4. The

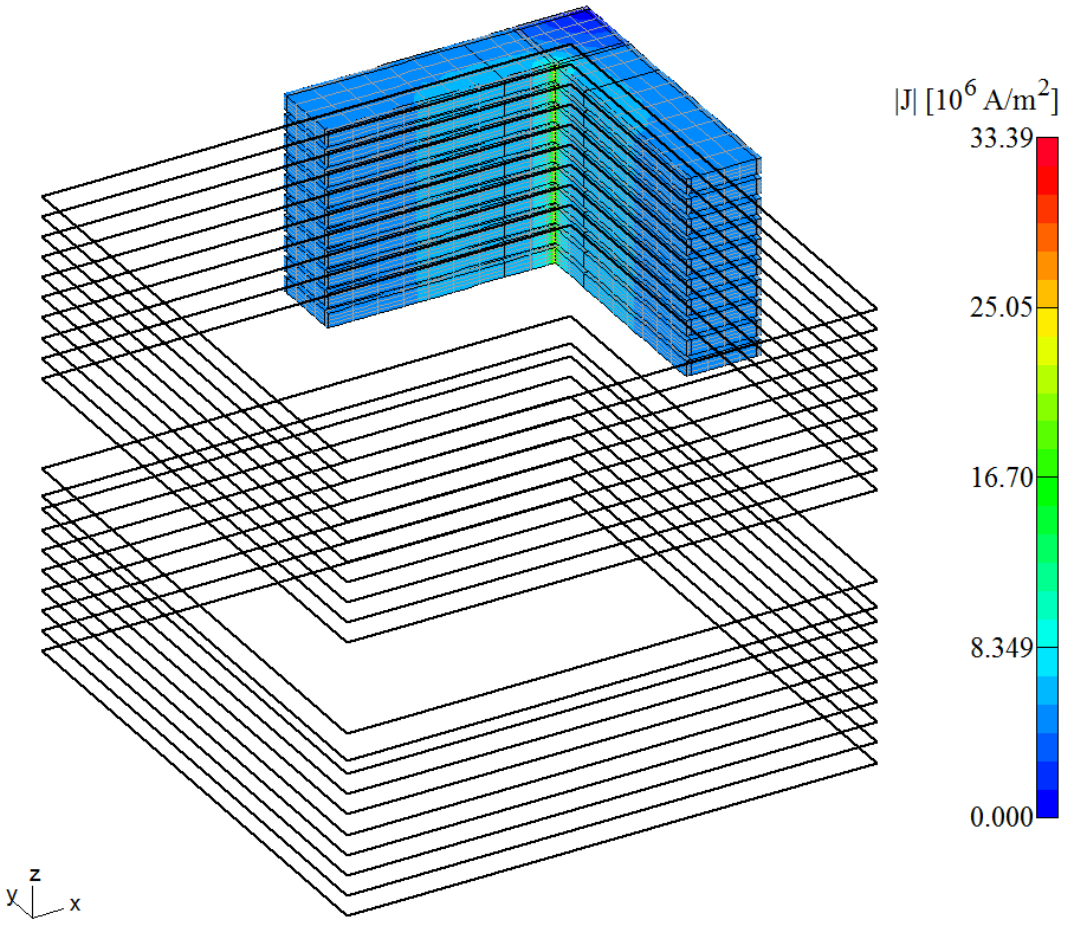

Figure 8.4 Absolute value of the temporary current density distribution obtained by solving a current flow problem for $T, \Phi - \Phi$ technique, showing the current filaments through the conductors

current distribution is almost uniform except at the sharp edges as a result of the static current flow. The current density peak can be observed at the inner corner of the top conductor. The current density distribution results of the skin effect problem

obtained with both of the formulations are shown in 8.5 and 8.6. In the skin effect problem, the density peak is about 20 times higher.

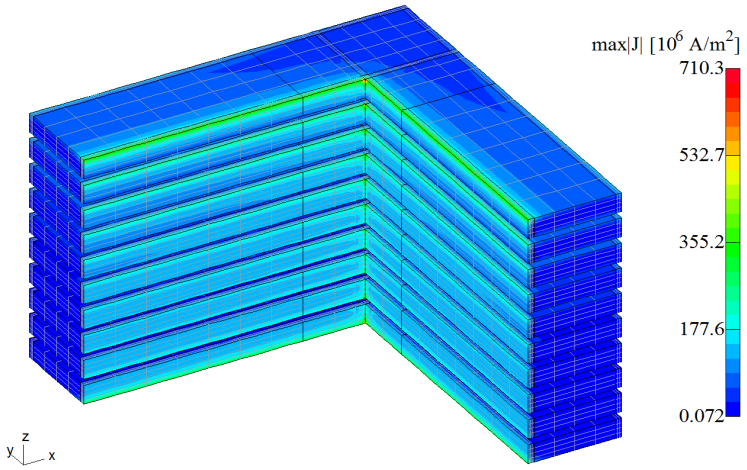

Figure 8.5 Absolute value of the current density distribution with $A, v - A$ technique

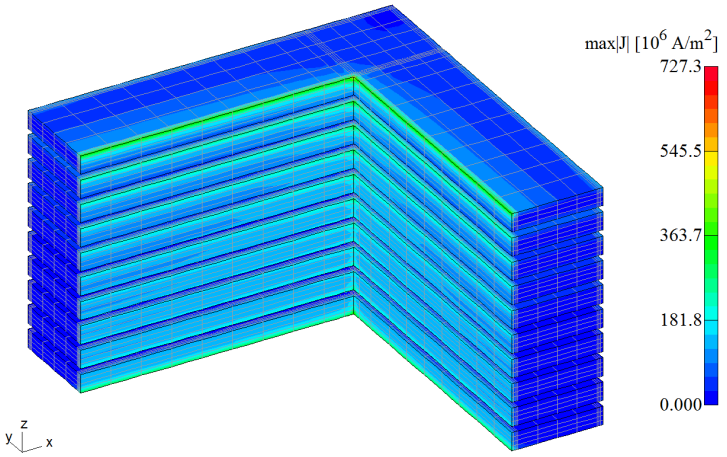

Figure 8.6 Absolute value of the current density distribution with $T, \Phi - \Phi$ technique

Cond.	$\mathbf{A}, v - \mathbf{A}$		$\mathbf{T}, \Phi - \Phi$	
No.	Force-X (kN)	Force-Z (kN)	Force-X (kN)	Force-Z (kN)
1	41.67	44.01	42.07	45.01
2	29.35	13.15	29.84	13.75
3	28.71	3.10	29.19	3.39
4	28.51	−6.26	28.99	−6.24
5	28.23	−15.38	28.71	−15.60
6	27.78	−24.62	28.27	−25.09
7	27.23	−34.30	27.71	−35.02
8	26.76	−44.55	27.24	−45.54
9	27.20	−54.90	27.72	−56.17
10	42.64	−79.64	43.12	−80.82

Method	**Energy (Joules)**	**Inductance (μH)**
$\mathbf{A}, v - \mathbf{A}$	346257.59	277.01
$\mathbf{T}, \Phi - \Phi$	345393.60	276.31

Table 8.1 Comparison of forces on the conductors, energy and inductance of the arrangement [2]

In Table 8.1, two of the three components of the forces acting on each of the turn, computed with both formulations, are compared. The forces in the x and y directions are of equal magnitude as is obvious from the problem symmetry. The electromagnetic energy and the inductance of the arrangement computed with both the techniques is also given in Table 8.1. This shows a good agreement.

Table 8.2 characterizes the computational resources. It is evident from the results that the $\mathbf{T}, \Phi - \Phi$ approach is more efficient as far as computational time is concerned. One reason is also shown in the table that the number of degrees of freedom are less in this approach due to the definition of the scalar potential in the whole problem domain. On the other hand the magnetic vector potential is defined in the whole problem region in the $\mathbf{A}, v - \mathbf{A}$ approach. Hence, due to the smaller problem size the solution time is lower in the $\mathbf{T}, \Phi - \Phi$ approach. But on the other hand, the additional resources such as considering the current filaments and solving the static current flow problem are required in this approach. The above problem is more evident when the conducting domain in the skin effect problem is multiply connected. The computational time for the impressed field is also restrictive when there is a large number of conductors with given currents involved in the problem.

Method	No. of DoF.	No. of CG it.	CPU time(seconds)
$\mathbf{A}, v - \mathbf{A}$	1187998	9126	11975
$\mathbf{T}, \Phi - \Phi$	525368	1719	876

Table 8.2 Comparison of computational data and results [2]

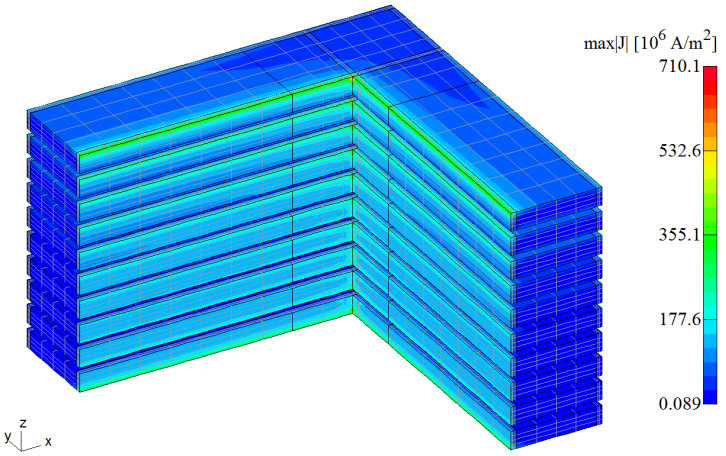

Figure 8.7 Absolute value of the maximum current density distribution with voltage prescription condition $A, v - A$ technique

8.1.3. Validation of results

Although the comparison of the results obtained with both the approaches validates the new technique developed, another reverse approach is also used to reinforce the validation argument. The voltage across the conductors is obtained in terms of the scalar potential in the $\mathbf{A}, v - \mathbf{A}$ formulation when the problem is solved with given current condition. These voltages are given in Table 8.3, with the numbering of inductors from bottom to top.

The so obtained potential values are then specified to solve the problem with the voltage prescription condition, which validates the results obtained by the given current condition of the same formulation. This result is presented in Fig. 8.7 which is similar to that in Fig. 8.5.

To observe the skin effect behaviour inside the conductor line graphs for the total current density are shown for both the techniques in Fig. 8.8 and Fig. 8.9. It is apparent that the current density is maximum on the inner side of the conductor which is due to the skin effect as well as in accordance with Ohm's law. However, the higher current density on the outer surface of the conductor as compared to the inner part is solely due to the skin effect.

No. of inductor	Voltage (Re)	Voltage (Im)
1	4.48	224.09
2	5.51	227.36
3	6.08	228.81
4	6.26	228.48
5	6.07	226.43
6	5.54	222.67
7	4.64	217.18
8	3.31	209.90
9	1.46	200.79
10	−1.03	189.88

Table 8.3 Voltages across inductors.

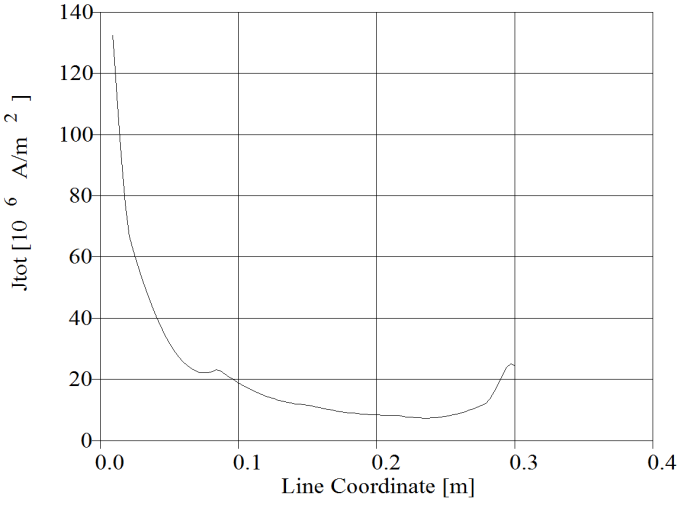

Figure 8.8 Skin effect shown for the bottom conductor at 55mm depth along the line of width $\mathbf{A}, v - \mathbf{A}$ technique

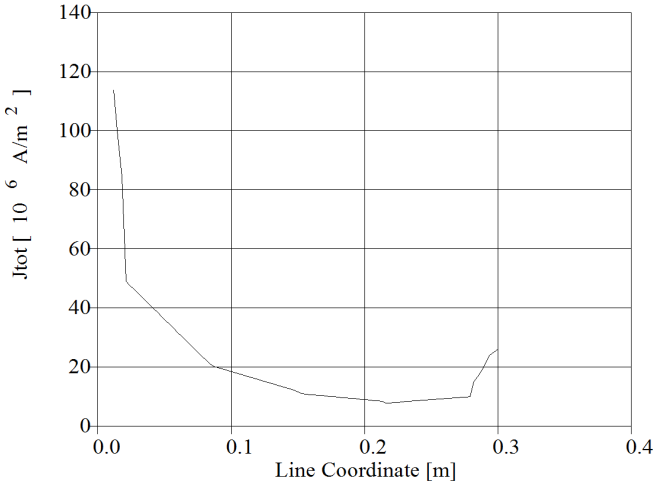

Figure 8.9 Skin effect shown for the bottom conductor at 55mm depth along the line of width $\mathbf{T}, \Phi - \Phi$ technique

8.2. Higher harmonic losses in an asynchronous machine

The reduction of the total loss of electrical machines is one of the most important research goals in machine design. The aim of this work has been to evaluate the copper loss in the short circuit ring using three dimensional (3D) finite element analysis (FEA). The stator winding is supplied with 3-phase supply at 50 Hz. The induced current in the rotor bars has a nonuniform distribution due to skin effect. The current density distribution and the resulting copper loss in the bars and the end ring are determined in this analysis.

This problem is solved using the $\mathbf{A}, v - \mathbf{A}$ formulation with prescribing the total current through the bars as presented in *chapter 6*. It is not possible to attempt this analysis with the $\mathbf{T}, \Phi - \Phi$ formulation because of the large number of inductors involved and the complex geometry of the problem conducting domain.
The subject of this work is to compute the additional losses in the rotor squirrel cage under open-circuit conditions. The end region of a 2.5 MW, 14 poles IM with 84 stator slots and 112 rotor bars is modeled for the higher harmonic losses in the end region.

Since the losses in the rotor bars can be evaluated using two dimensional (2D) finite element analysis, the comparison of the two analyses was also carried out. The losses that arise in the short circuit ring, can not be estimated by a 2D analysis. The main purpose of the 3D analysis was to determine the eddy current losses which occur at several harmonics in the end ring to which the rotor bars are connected.

8.2.1. 3D model of the motor end region

A 3D model of the end region of the machine is built using ANSYS [57]. A nonuniform mesh is required to take account of the skin effect in the conducting domain. The 2D model is built first and the FE mesh is generated taking into account the skin depth of the conducting material at higher frequencies. A portion of the 2D model is shown in Fig. 8.10, which is extruded into the 3rd dimension afterwards. A length of $30cm$ on both sides of the end ring, i.e. on bars side and on the end air region, is modeled. The complete model consists of 314730 hexahedral elements. A portion of the 3D model and its mesh are shown in Fig. 8.11. The model was built to take into account the stator excitation and definition of the properties of stator and rotor iron, so that it was possible to study the effects of different parameters.

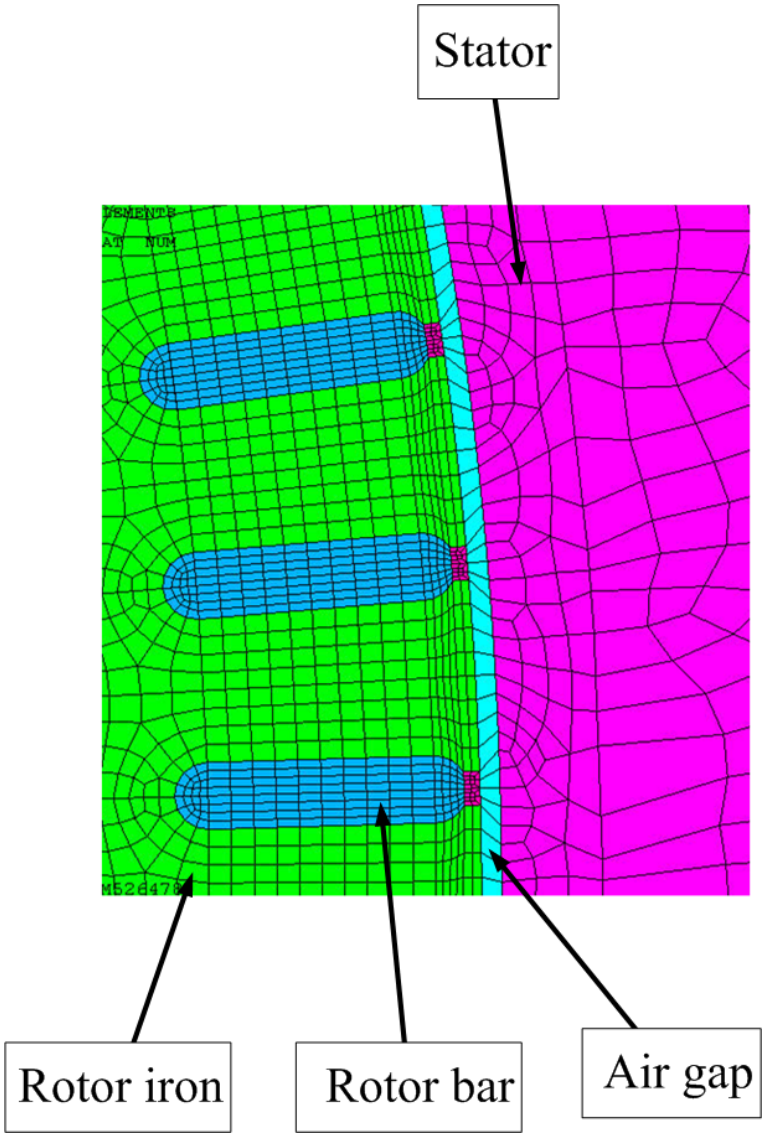

Figure 8.10 2D model of the motor and mesh

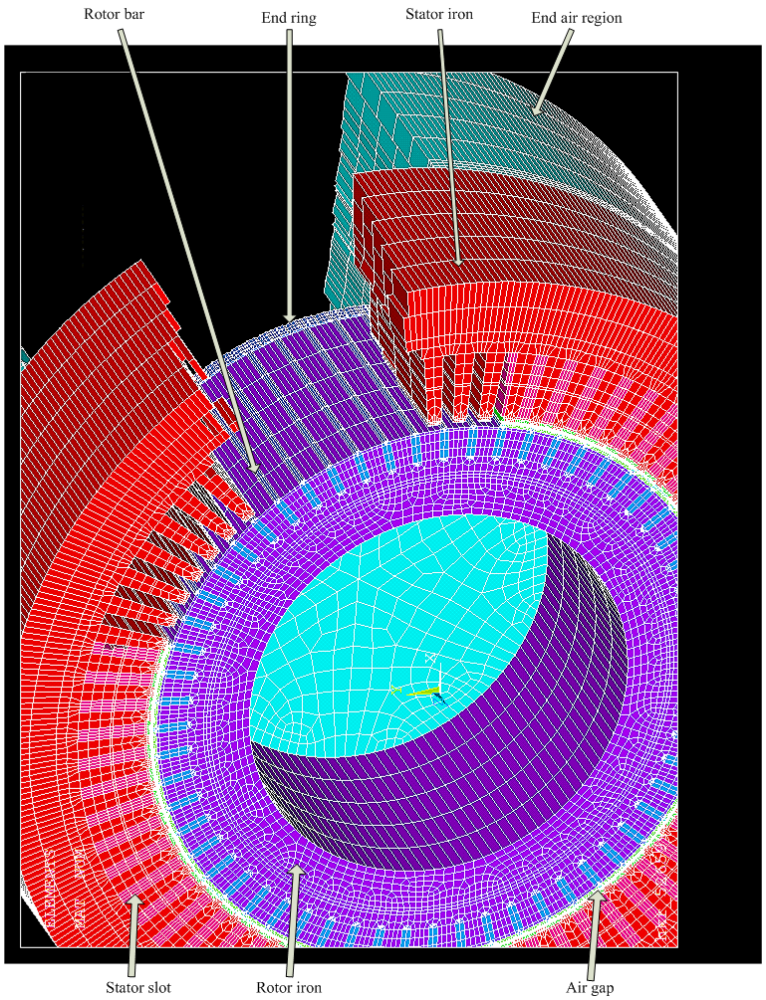

Figure 8.11 Portion of the motor 3D model and mesh

8.2.2. Computation of rotor currents

A 2D numerical simulation using a single component magnetic vector potential and with motion of the rotor taken into consideration in order to evaluate the copper losses in the rotor slots was performed. As a result of this transient analysis, the rotor currents have become available which are required to be prescribed for different higher harmonics in the 3D analysis. The rotor movement has been realized in the 2D transient computation using a time-stepping procedure where the geometry modification due to rotor rotation in every time-step has been considered by linear interpolation along the sliding interface in the air-gap [58]. The time increment between the transient steps has been small enough to take the stator slot's harmonics into consideration:

$$\nu = p + gN_1 \quad \text{with } g = \pm 1, \pm 2, \cdots \tag{8.1}$$

where ν denotes the spatial harmonic order, p stands for the number of stator pole pairs ($p = 7$) and N_1 for the number of stator slots ($N_1 = 84$). These spatial harmonics of the stator field induce the rotor currents with the rotor frequency

$$f_\nu^R = \left[\frac{f_\nu^S}{f_1} - (1 - s) \frac{\nu}{p} \right] f_1 \tag{8.2}$$

where f_ν^S denotes the frequency of the spatial field wave in the stator coordinate system, s is the slip ($s = 0$) and f_1 stands for the nominal frequency of $50Hz$. Hence, dominating rotor currents of frequencies of $300Hz$, $600Hz$, $1200Hz$ and higher are to be expected. In order to discretize the current period of a frequency of $1200Hz$ by more than 10 samples, a time-step of $50\,\mu s$ has been employed.

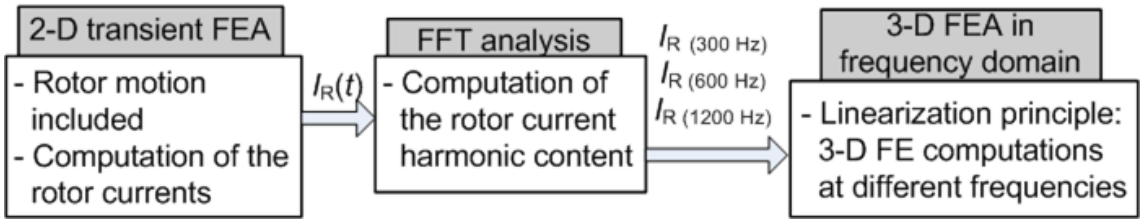

Figure 8.12 Flowchart of the proposed procedure. [1]

Using the procedure of Fig. 8.12, the losses in the rotor bars have been evaluated. The losses that arise in the short circuit ring, through which the rotor conductors are connected, can not be estimated by a 2D analysis. In order to evaluate these losses, a 3D FE simulation is required. Since a transient 3D analysis with the included motion would require an enormous amount of calculation time, the simulation has been carried out in the frequency domain. Separate simulations for the three prominent harmonics have been carried out. The model has been linearized and the superposition principle has been applied to determine the higher harmonic losses cumulatively.

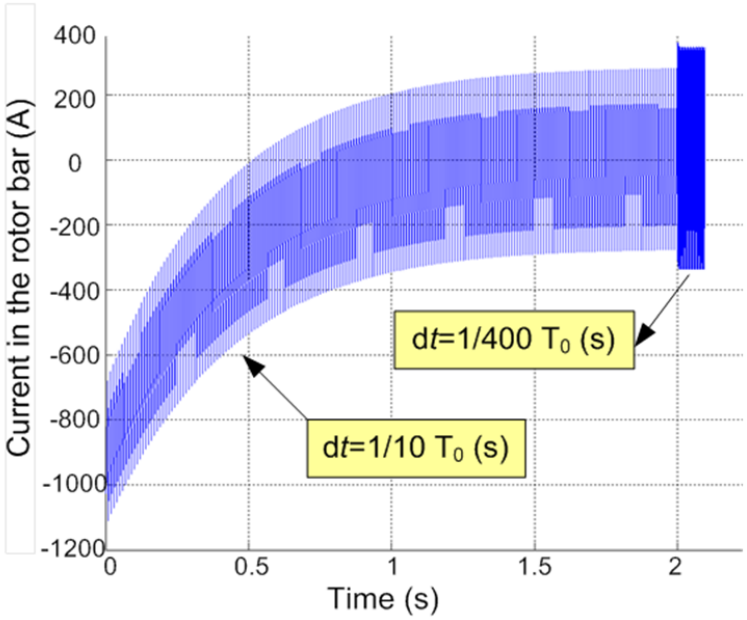

Figure 8.13 Current in the rotor bar obtained by transient 2-D FE analysis. [1]

8.2.3. 3D analysis

By analyzing the harmonic content of the currents obtained by 2D simulation, the individual rotor current harmonics have been separately prescribed in the 3D analysis. The 3D simulation has been carried out using the $\mathbf{A}, v-\mathbf{A}$ formulation in the frequency domain. The detail of the new feature of this formulation has been given in *chapter 6*.

8.2.3.1. Boundary conditions

Boundary conditions for the problem were specified at the bounding surfaces of the outer elements of the model. There is neither a far boundary nor a magnetic symmetry plane. Only one electric symmetry plane is present where a non homogeneous boundary condition for the electrodes with the given current condition is present. In this model, the normal component of the magnetic flux density is assumed to vanish on the round surface, i.e. around the stator iron and end air region. Therefore the tangential component of the magnetic vector potential is zero there. Furthermore, at the end of the end air region the similar condition is applicable. The number of electrodes with the given current condition are 112 in this problem. For each harmonic analysis the currents to be prescribed have been obtained as shown earlier. Each harmonic present in the currents obtained by 2D transient analysis has been prescribed to one 3D model.

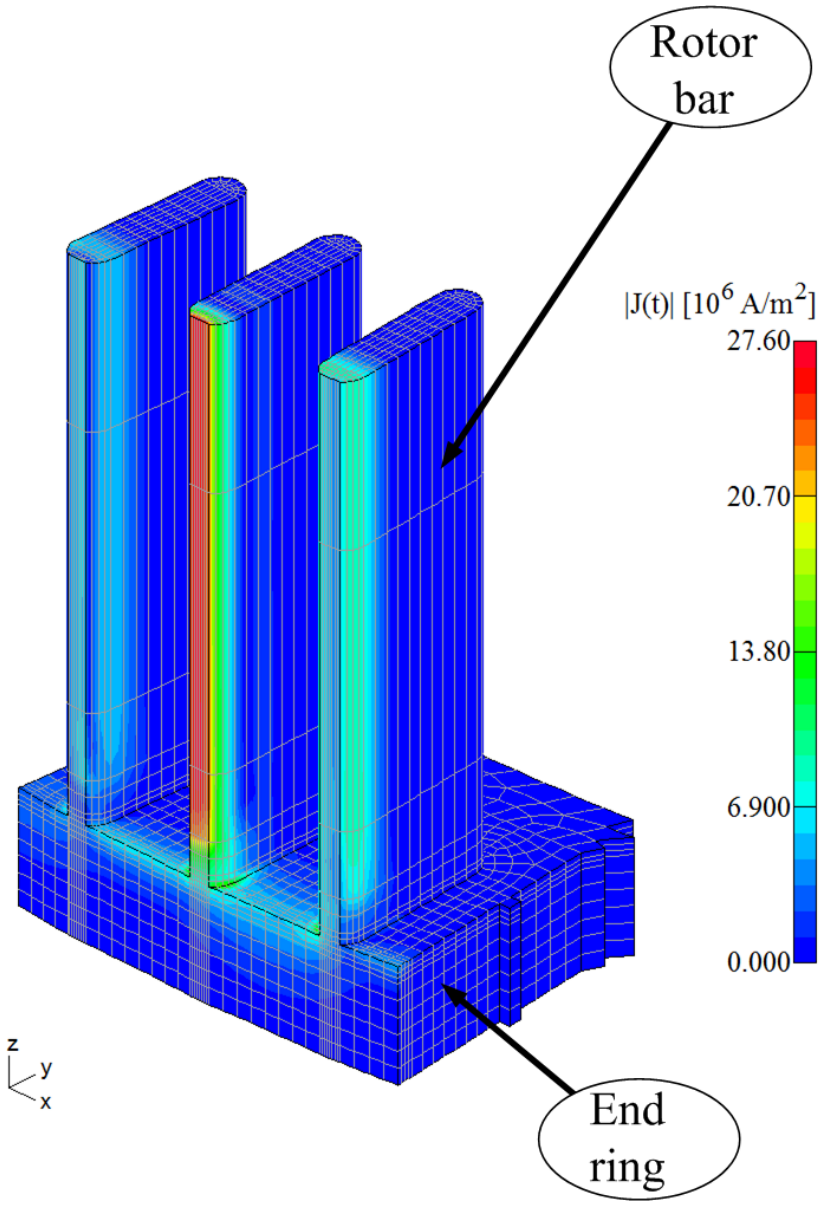

Figure 8.14 Current density distribution in the portion of the end-ring at $600Hz$ [1]

Type of the analysis	Calculated losses
3D Harmonic analysis at 300 Hz (first winding field)	0.6%
3D Harmonic analysis at 600 Hz (first stator slot harmonic)	96.8%
3D Harmonic analysis at 1200 Hz (second stator slot harmonic)	0.8%
Sum of all losses obtained by 3D harmonic analysis	98.2%
Transient analysis (2D)	100%

Table 8.4 Comparison of the losses in rotor bars obtained by 2D transient and by 3D harmonic analysis [1].

8.2.3.2. Results

The current density distribution obtained in the analysis is shown in a portion of the end-ring and connecting rotor bars in Fig. 8.14. It can be observed that a peak occurs in the rotor bar. The portion of the bars that is outside the rotor iron has a remarkably low current density. The current density field is even more uniform in the end-ring. It can be anticipated that more copper losses occur in the bars as compared to the short circuit ring.

As seen from Table 8.4, using this proposed procedure, the losses in the rotor slots obtained by transient 2D analysis and losses obtained by harmonic 3D analysis are in good agreement. Based on these results the assumption can be made that the superposition principle is an acceptable method in order to reduce the computation time.

Excess rotor copper losses in the rotor end-ring have been computed using a generalized $\mathbf{A}, v - \mathbf{A}$ formulation and the superposition principle for higher harmonics of the rotor current. It has been shown that, using this proposed numerical procedure, the excess rotor copper losses can be evaluated in the frequency instead of in the time domain. For each frequency of the rotor current, an equation system of 14 millions unknowns has been solved. The solving procedure carried out in the single core of a $2.8\,GHz$ personal computer with 36 GB RAM took approximately 3 days. It has been proven that excess rotor copper losses in the rotor bars can present a very prominent loss component. These parasitic effects can only be reduced by altering the stator slot number or by redesigning the rotor slot geometry. On the other hand, based on the results of this research, the conclusion can be drawn that the copper losses in the rotor end-ring are much smaller compared to rotor bars and do not provoke considerable heating of the induction machine.

Table 8.4 shows the losses in the rotor bars computed at the three important harmonics in 3D analysis and those obtained through 2D transient analysis. It is interesting to note that the losses computed in the rotor bars are higher as a result of 2D analysis than those obtained in the 3D one. The reason is that 2D transient analysis take account all higher harmonics whereas in 3D analysis losses due to selected harmonics are

computed only. Another reason is taking account of the nonlinearity which is neglected in 3D computation. A linear ferromagnetic material is considered ($\mu = 1000$) for all computations.

8.2.3.3. Leakage inductance approximation of the end ring

The inductance plays an important role in the characterization of magnetic devices such as motors. In the foregoing analysis of the induction motor, the leakage inductance of the end ring is approximated using the magnetic energy in the end region. The relationship

$$W = \sum_{i=1}^{n} \frac{1}{2} \left(L_{ER} I_{ER}^2 \right) \tag{8.3}$$

is used for this computation, where L_{ER} is the leakage inductance of the portion of the end ring between two bars and n the number of rotor bars. I_{ER} is the current in the end-ring which is obtained through the 3D analysis by integrating the current density field at a cross section of the end-ring between the two bars.
Inductance with the axisymmetric 2D model shown in the Fig. 8.15 is also computed for the comparison purpose. The two results are in good agreement.

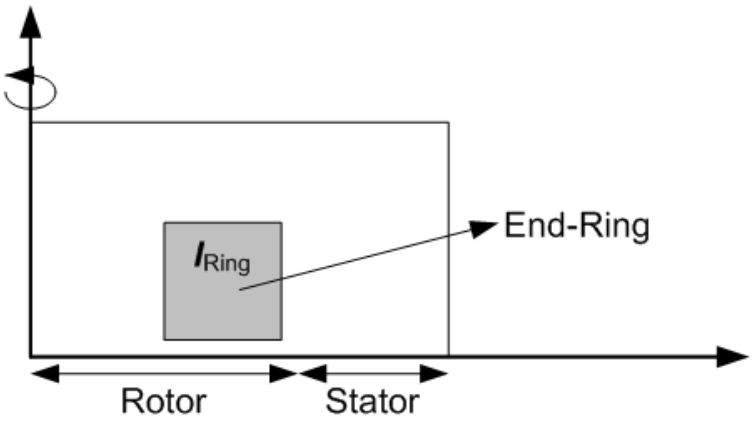

Figure 8.15 Axi-symmetric 2D model of the end-ring

8.3. Transient analysis of the multi turn reactor coil problem

The problem of section 8.1 has been studied for its transient behaviour with prescribed sinusoidal current at 50 Hz frequency. The motivation behind the choice of the above problem was to verify the implementation of the given current feature of the $\mathbf{A}, v - \mathbf{A}$ formulation for transient skin effect problems. Since the frequency domain analysis results are already available, the verification goal is economically achieved. The new feature is validated only for linear problems, although it is implemented for nonlinear problems too.

The problem is solved with three approaches, first with the time stepping method, second in the discrete frequency domain by the backward Euler method using constant time step, and third with the harmonic balance method in the frequency domain.

8.3.1. Time stepping

The time stepping solution takes a long time due to the large time constant of the equivalent circuit of the inductor arrangement. In fact, it was expected beforehand that the solution time will be long to obtain the steady state solution with the time stepping procedure. On the basis of the post processing results of the problem solution in the frequency domain the estimated time constant of the reactor arrangement is $0.1636\,s$. The time to reach the steady state is usually five times the time constant. This means that, for the excitation of the 50 Hz, the expected steady state solution will be available after stepping through 41 periods. The transient results of the reactor arrangement problem, which can be represented as an equivalent RL circuit, verified this behaviour afterwards. The current density distribution at the specific time instants are shown in Figs. 8.16, 8.17 and 8.18. A time step of 2 ms was chosen for the first 30 periods and 1 ms for stepping though the last 14 periods. After stepping through about 40 cycles the periodicity condition is satisfied approximately.

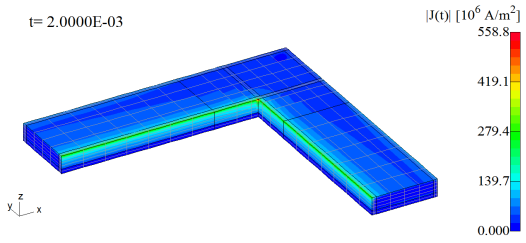

Figure 8.16 Current density field peak value in the top conductor at time 2 ms

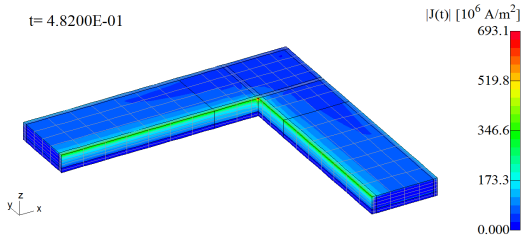

Figure 8.17 Current density field peak value in the top conductor at time 482 ms

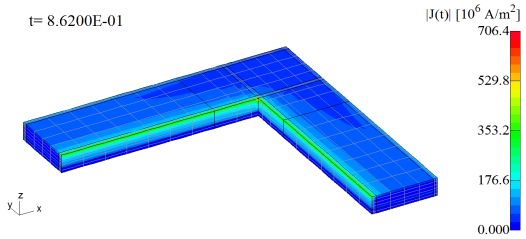

Figure 8.18 Current density field peak value in the top conductor at time 862 ms

8.3.2. Harmonic solution in the time domain

Since the prescribed current is time harmonic, the time stepping is not necessary when we are interested in the steady state solution of the transient skin effect problem only. Enforcing the periodicity condition and using the discrete Fourier transform the solution is obtained by stepping through one period.
It can be observed that with the use of fine time step the steady state solution is more close to the solution obtained in the frequency domain analysis as in section 8.1. The current density peak occurs in the top most conductor, therefore the results are shown for three different time discretizations, i.e. 36, 60 and 200 time steps in one period.

The current density distribution is shown in Figs. 8.19, 8.20 and 8.21 for the corresponding time instant of 0.002 sec or 0.012 sec which may be compared with the solution in the time harmonic case shown in Fig. 8.5 which occurs at an electrical angle of 127°.
The steady state solution was achieved in about 35 days using the time stepping technique for this problem, whereas the discrete frequency approach took only 6.5 *hours* with 200 time steps in one period on the same machine.

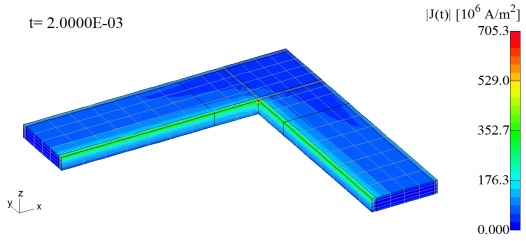

Figure 8.19 Current density field peak value (occur at 0.002s) in the discrete frequency analysis with 36 time steps

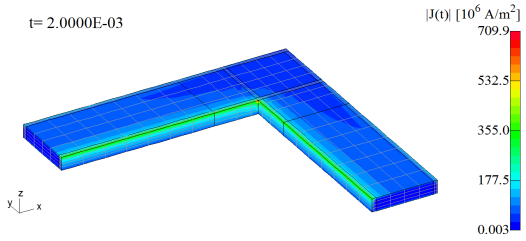

Figure 8.20 Current density field peak value (occur at 0.002s) in the discrete frequency analysis with 60 time steps

8.3.3. Harmonic solution in the frequency domain

Since the problem is linear, the higher harmonics are not expected in the solution. The current prescribed condition is given for the $50Hz$ excitation at the electrodes and 36 discrete time steps are defined using the harmonic balance scheme. The problem is solved in 9172 Conjugate Gradient iterations. The current density plot is shown in Fg. 8.22

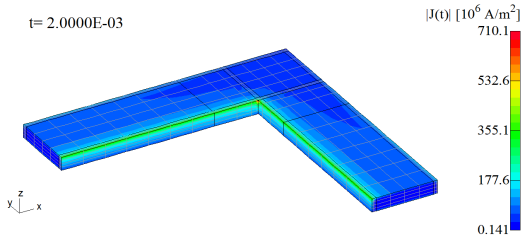

Figure 8.21 Current density field peak value (occur at 0.002s) in the discrete frequency analysis with 200 time steps

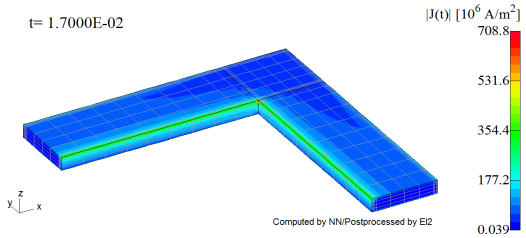

Figure 8.22 Current density field peak value (occur at 0.017s) in the harmonic balance method

Chapter 9

Conclusion

In this work, the emphasis was put on the treatment and incorporation of the current prescription condition in the $\mathbf{A}, v-\mathbf{A}$ potential formulation for the skin effect problem. After presenting a brief literature review of finite element techniques developed for this class of problems, the Galerkin method was explained with reference to the two specific formulations. Next, focus was made to compare two dual formulations, the $\mathbf{A}, v-\mathbf{A}$ and the $\mathbf{T}, \Phi-\Phi$ for both the voltage and the current prescription conditions.

It was shown that the voltage prescription condition is a strong global constraint for the magnetic vector potential formulation. The given voltage condition is satisfied by enforcing the corresponding scalar potential value on the respective electrodes as an essential boundary condition.

In contrast, the current prescription condition is a strong global constraint for the current vector potential formulation. It is satisfied through the introduction of the impressed field function which represent the Biot-Savart field in the eddy current free domain, whereas in the conducting domain, its curl represents an arbitrary current density distribution and is defined by the solution of the stationary current flow problem. The tangential component of the impressed field function is set equal to the tangential component of the Biot-Savart filed on the interface of the conducting and nonconducting domains. Consequently, the given current condition is satisfied for the skin effect problem. The computational requirements of the impressed field function limits this formulation to skin effect problems with low number of inductors. The necessity to take account of the multiply connected conducting domain is also a limitation of this formulation.

In the $\mathbf{T}, \Phi-\Phi$ formulation voltage sources require the introduction of a source field function. The computation of the Biot-Savart field and the solution of the stationary current flow problems are also prerequisites to solve the skin effect problem with a general multiply connected conducting domain.

In the $\mathbf{A}, v - \mathbf{A}$ formulation, the given current condition of the skin effect problem is treated as a periodic boundary condition to be satisfied essentially.

General time dependent skin effect problems with given current condition are solved with time stepping technique. The prescribed current is discretized and incorporated for the additional equations arising in case of $\mathbf{A}, v - \mathbf{A}$ formulation. The special case of time periodic excitation is dealt with both in frequency domain, with harmonic balance method, and in discrete frequency domain, with backward Euler method with constant time step.

Industrial applications have been included to show the capabilities as well as the merits and demerits of both the formulations in different special situations, after presenting relatively simple problems solved with both the formulations for comparison of computational effort. It has been shown that the $\mathbf{T}, \Phi - \Phi$ formulation is preferable for the current prescription condition due to its advantage of less computational time, and, hence a lower number of resulting degrees of freedom, when the problem domain is simply connected (or at least with low number of holes) or with a small number of inductors. On the other hand, when there is a large number of inductors involved with the current prescription condition or the skin effect problem involves the prescribed voltage condition, the $\mathbf{A}, v - \mathbf{A}$ formulation is better suited.

Chapter A

Appendix

A.1. Node based 3-D shape functions

Twenty second order (in each of the three variables) polynomials, $N_k^{(e)}(\xi,\eta,\zeta)$ are used to approximate the potentials. These are called shape functions of the Serendipity class (Horace Walpole), due to their discovery by chance and can be written in a closed form.

For Corner Nodes $(\xi=\pm1,\eta=\pm1,\zeta=\pm1)$:

$$N_k^{(20)}(\xi,\eta,\zeta)=\frac{1}{8}(1\pm\xi)(1\pm\eta)(1\pm\zeta)(\pm\xi\pm\eta\pm\zeta-2),\ k=1,2,\cdots,20. \tag{A.1}$$

For Side middle Nodes:

$$N_k^{(20)}(\xi,\eta,\zeta)=\frac{1}{4}(1-\xi^2)(1\pm\eta)(1\pm\zeta),\quad \xi=0,\eta=\pm1,\zeta=\pm1, \tag{A.2}$$

$$N_k^{(20)}(\xi,\eta,\zeta)=\frac{1}{4}(1\pm\xi)(1-\eta^2)(1\pm\zeta),\quad \xi=\pm1,\eta=0,\zeta=\pm1, \tag{A.3}$$

$$N_k^{(20)}(\xi,\eta,\zeta)=\frac{1}{4}(1\pm\xi)(1\pm\eta)(1-\zeta^2),\quad \xi=\pm1,\eta=\pm1,\zeta=0, \tag{A.4}$$

$$k=1,2,\cdots,20.$$

A.2. Edge based 3-D shape functions

In Fig. 1.1, the orientation of the edges of one vector finite element is shown. 12 of the 36 edges are in one coordinate direction, therefore the shape functions which are the second order polynomials, for only ξ direction are written here. The basis functions,

in other two directions can be obtained by cyclic interchange of the local variables, ξ, η and ζ.

$$\mathbf{N}_k^{(36)}(\xi,\eta,\zeta) = \frac{1}{8}(1+\eta_k\eta)(1+\zeta_k\zeta)(4\xi_k\xi+\eta_k\eta+\zeta_k\zeta-1)grad\xi, \quad k=1,2,\cdots,8, \tag{A.5}$$

where $\xi_k = \pm\frac{1}{2}$, $\eta_k = \pm 1$ and $\zeta_k = \pm 1$,

$$\mathbf{N}_k^{(36)}(\xi,\eta,\zeta) = \frac{1}{4}(1-\eta^2)(1+\zeta_k\zeta)grad\xi, \quad k=9,12 \qquad \zeta_k=\pm 1, \tag{A.6}$$

$$\mathbf{N}_k^{(36)}(\xi,\eta,\zeta) = \frac{1}{4}(1+\eta_k\eta)(1-\zeta^2)grad\xi, \quad k=10,11 \qquad \eta_k=\pm 1. \tag{A.7}$$

Bibliography

[1] Stermecki, A. and Biro, O. and Bakhsh, I. and Rainer, S. and Ofner, G. and Ingruber, R., "3-D Finite Element Analysis of Additional Eddy Current Losses in Induction Motors," *Magnetics, IEEE Transactions on*, vol. 48, no. 2, pp. 959 –962, Feb. 2012.

[2] I. Bakhsh, O. Bíró, and K. Preis, "Skin effect problems with prescribed current condition," in *14th International IGTE Symposium on Numerical Field Calculation in Electrical engineering, Graz, Austria*, 2010, pp. 249–254.

[3] J. G. V. Bladel, *Electromagnetic Fields*. 685 Canton Street Norwood, MA 02062: John Wiley & Sons, Inc., 2007.

[4] D. J. Griffiths, *Introduction to Electrodynamics*, 3rd ed. Upper Saddle River, New Jersey 07458: Prentice-Hall, 1999.

[5] A. Bossavit, *Computational Electromagnetism Variational Formulations, Complementarity, Edge elements*. USA: Academic Press, 1998.

[6] A. A. Rodríguez and A. Valli, *Eddy Current Approximation of Maxwell Equations Theory, algorithms and applications*. New York: Springer-Verlag, 2010.

[7] Biro, O. and Preis, K., "An efficient time domain method for nonlinear periodic eddy current problems," *Magnetics, IEEE Transactions on*, vol. 42, no. 4, pp. 695 –698, April 2006.

[8] P. P. Silvester and R. L. Ferraari, *Finite elements for electrical engineers*, 3rd ed. 685 Canton Street Norwood, MA 02062: Cambridge University Press, 1996.

[9] O. Bíró and K. R. Richter, "CAD in Electromagnetism," *P. W. Hawkes (ed), Advances in Electronics and Electron Physics*, vol. 82, pp. 1–96, 1991.

[10] O. Bíró and K. Preis, "On the use of the magnetic vector potential in the finite-element analysis of three-dimensional eddy currents," *Magnetics, IEEE Transactions on*, vol. 25, no. 4, pp. 3145 –3159, Jul 1989.

[11] O. Bíró, "Edge element formulations of eddy current problems," *Computer Methods in Applied Mechanics and Engineering*, vol. 169, no. 3-4, pp. 391 – 405, 1999.

[12] R. Garg, *Analytical and Computational Methods in Electromagnetics*. 685 Canton Street Norwood, MA 02062: Artech House, Inc., 2008.

[13] P. Silvester, "The accurate calculation of skin effect in conductors of complicated shape," *Power Apparatus and Systems, IEEE Transactions on*, vol. PAS-87, no. 3, pp. 735 –742, March 1968.

[14] S. R. H. Hoole., *Computer-aided analysis and design of electromagnetic devices*. New York: Elsevier, 1989.

[15] P. Silvester, "Skin effect in multiple and polyphase conductors," *Power Apparatus and Systems, IEEE Transactions on*, vol. PAS-88, no. 3, pp. 231 –238, March 1969.

[16] K. H. Huebner, *The Finite Element Method for Engineers*. Hemel Hempstead, United Kingdom: John Wiley & Sons, Inc., 1975.

[17] G. R. LIU and S. S. QUEK, *The Finite Element Method A practical course*. Toronto: Butterworth-Heinemann, 2003.

[18] e. M.V. K. Chari, *Finite Elements in electrical and Magnetic Field Problems*, 1st ed., M. V. K. C. P. P. Silvester, Ed. NY, USA: John Wiley & Sons, Ltd., 1980.

[19] A. Konrad, M. Chari, and Z. Csendes, "New finite element techniques for skin effect problems," *Magnetics, IEEE Transactions on*, vol. 18, no. 2, pp. 450 – 455, Mar. 1982.

[20] I. Mayergoyz, "A new approach to the calculation of three-dimensional skin effect problems," *Magnetics, IEEE Transactions on*, vol. 19, no. 5, pp. 2198 – 2200, Sep. 1983.

[21] P. Leonard, D. Rodger, and R. Hill-Cottingham, "Calculation of AC losses in current forced conductors using 3D finite elements and the $\mathbf{A}\psi$V method," *Magnetics, IEEE Transactions on*, vol. 26, no. 2, pp. 490 –492, Mar 1990.

[22] O. Bíró, K. Preis, W. Renhart, G. Vrisk, and K. Richter, "Computation of 3-d current driven skin effect problems using a current vector potential," *Magnetics, IEEE Transactions on*, vol. 29, no. 2, pp. 1325 –1328, Mar. 1993.

[23] S. Bouissou and F. Piriou, "Study of 3d formulations to model electromagnetic devices," *Magnetics, IEEE Transactions on*, vol. 30, no. 5, pp. 3228 –3231, Sep. 1994.

[24] O. Bíró and K. Preis, "Finite element analysis of 3-d eddy currents," *Magnetics, IEEE Transactions on*, vol. 26, no. 2, pp. 418 –423, Mar. 1990.

[25] O. Bíró, K. Preis, and K. Richter, "On the use of the magnetic vector potential in the nodal and edge finite element analysis of 3d magnetostatic problems," *Magnetics, IEEE Transactions on*, vol. 32, no. 3, pp. 651 –654, May 1996.

[26] P. Dular, F. Henrotte, and W. Legros, "A general and natural method to define circuit relations associated with magnetic vector potential formulations," *Magnetics, IEEE Transactions on*, vol. 35, no. 3, pp. 1630 –1633, May 1999.

[27] P. Dular, C. Geuzaine, and W. Legros, "A natural method for coupling magnetodynamic h-formulations and circuit equations," *Magnetics, IEEE Transactions on*, vol. 35, no. 3, pp. 1626 –1629, May 1999.

[28] P. Dular, P. Kuo-Peng, C. Geuzaine, N. Sadowski, and J. Bastos, "Dual magnetodynamic formulations and their source fields associated with massive and stranded inductors," *Magnetics, IEEE Transactions on*, vol. 36, pp. 1293 –1299, 2000.

[29] P. Dular, A. Genon, J.-Y. Hody, W. Legros, J. Mauhin, and A. Nicolet, "Coupling between edge finite elements, nodal finite elements and boundary elements for the calculation of 3-d eddy currents," *Magnetics, IEEE Transactions on*, vol. 29, no. 2, pp. 1470 –1474, Mar. 1993.

[30] P. Dular, J.-F. Remacle, F. Henrotte, A. Genon, and W. Legros, "Magnetostatic and magnetodynamic mixed formulations compared with conventional formulations," *Magnetics, IEEE Transactions on*, vol. 33, no. 2, pp. 1302 –1305, Mar. 1997.

[31] R. Jafari-Shapoorabadi, A. Konrad, and A. Sinclair, "Comparison of three formulations for eddy-current and skin effect problems," *Magnetics, IEEE Transactions on*, vol. 38, no. 2, pp. 617 –620, Mar. 2002.

[32] S. Alfonzetti, "Finite-element mesh adaptation of 2-d time-harmonic skin effect problems," *Magnetics, IEEE Transactions on*, vol. 36, no. 4, pp. 1592 –1595, Jul. 2000.

[33] D. Prof. RNDr Karel Rektorys, *Variational Methods in Mathematics, Science and Engineering*, 2nd ed. Czechoslovakia by SNTL, Prague: D. Reidel Publishing Company, 1977.

[34] O. Bíró, "Use of a two-component vector potential for 3-d eddy current calculations," *Magnetics, IEEE Transactions on*, vol. 24, no. 1, pp. 102 –105, Jan. 1988.

[35] G. Paoli, "Nonlinear time harmonic 3D eddy current problems," Ph.D. dissertation, Technical University of Graz, May 1998.

[36] A. Bossavit, "Solving maxwell equations in a closed cavity, and the question of 'spurious modes'," *Magnetics, IEEE Transactions on*, vol. 26, no. 2, pp. 702 –705, Mar. 1990.

[37] B. D. Bartolo, *Classical Theory of Electromagnetism*, 2nd ed. 5 Toh Tuck Link, Singapore 596224: World Scientific, 2004.

[38] J. Coulomb, G. Meunier, and J. Sabonnadiere, "Energy methods for the evaluation of global quantities and integral parameters in a finite elements analysis of electromagnetic devices," *Magnetics, IEEE Transactions on*, vol. 21, no. 5, pp. 1817 – 1822, Sep. 1985.

[39] O. Bíró, P. B hm, K. Preis, and G. Wuchtka, "Edge finite element analysis of transient skin effect problems," *Magnetics, IEEE Transactions on*, vol. 36, pp. 835–839, 2000.

[40] Bossavit, Alain, "A rationale for 'edge-elements' in 3-D fields computations," *Magnetics, IEEE Transactions on*, vol. 24, no. 1, pp. 74 –79, jan 1988.

[41] O. Bíró, K. Preis, G. Vrisk, K. Richter, and I. Ticar, "Computation of 3-d magnetostatic fields using a reduced scalar potential," *Magnetics, IEEE Transactions on*, vol. 29, no. 2, pp. 1329 –1332, Mar. 1993.

[42] Z. Cendes, "Vector finite elements for electromagnetic field computation," *Magnetics, IEEE Transactions on*, vol. 27, no. 5, pp. 3958 – 3966, Sep. 1991.

[43] Oszkár Bíró and Preis, K., "Generating Source Field Functions With Limited Support for Edge Finite-Element Eddy Current Analysis," *Magnetics, IEEE Transactions on*, vol. 43, no. 4, pp. 1165 –1168, April 2007.

[44] O. Bíró, K. Preis, G. Buchgraber, and I. Ticar, "Voltage-driven coils in finite-element formulations using a current vector and a magnetic scalar potential," *Magnetics, IEEE Transactions on*, vol. 40, no. 2, pp. 1286 – 1289, 2004.

[45] G. Meunier, Y. Le Floch, and C. Guerin, "A nonlinear circuit coupled $\mathbf{t} - \mathbf{t_0} - \phi$ formulation for solid conductors," *Magnetics, IEEE Transactions on*, vol. 39, no. 3, pp. 1729 – 1732, May 2003.

[46] K. H. H. De Gersem, R. Belmans, "Floating potential constraints and field-circuit couplings for electrostatic and electrokinetic finite element models," *COMPEL: The International Journal for Computation and Mathematics in Electrical and Electronic Engineering*, vol. 22, no. 1, pp. 20–29, 2003.

[47] P. Dular, W. Legros, and A. Nicolet, "Coupling of local and global quantities in various finite element formulations and its application to electrostatics, magnetostatics and magnetodynamics," *Magnetics, IEEE Transactions on*, vol. 34, no. 5, pp. 3078 –3081, Sep. 1998.

[48] P. Bohm and G. Wachutka, "Numerical analysis tool for transient skin effect problems," in *Power Electronics Specialists Conference, 2004. PESC 04. 2004 IEEE 35th Annual*, vol. 2, 2004, pp. 880 – 884 Vol.2.

[49] O. Zienkiewicz and R. L. Taylor, *The Finite Element Method*, 5th ed. Butterworth-Heinemann, 2000, vol. Volume 1: The Basis.

[50] A. Kameari, "Calculation of transient 3d eddy current using edge-elements," *Magnetics, IEEE Transactions on*, vol. 26, no. 2, pp. 466 –469, Mar. 1990.

[51] P. of ISEF 05, *Electromagnetic Fields in Mechanics, Electrical and Electronic Engineering*, A. Krawczyk, Ed. Nieuwe Hemweg 6B, 1013 BG Amsterdam, Netherlands: IOS Press, 2006.

[52] Albanese, R. and Coccorese, E. and Martone, R. and Miano, G. and Rubinacci, G., "On the numerical solution of the nonlinear three-dimensional eddy current problem," *Magnetics, IEEE Transactions on*, vol. 27, pp. 3990–3995, 1991.

[53] Bíró, O. and Koczka, G. and Preis, K., "Fast Time-Domain Finite Element Analysis of 3-D Nonlinear Time-Periodic Eddy Current Problems With $\mathbf{T}$, $\Phi - \Phi$ Formulation," *Magnetics, IEEE Transactions on*, vol. 47, no. 5, pp. 1170 –1173, May 2011.

[54] S. Außerhofer, "An efficient harmonic balance method for nonlinear eddy-current problems," *IEEE Trans. on Magnetics, IEEE Transactions on*, vol. 43, no. 4, pp. 1229–1232, April 2007.

[55] Gergely Koczka, Stefen Außerhofer, Oszkár Bíró and Kurt Preis, "Fixed-point method for solving non linear periodic eddy current problems with $\mathbf{T}$, $\Phi - \Phi$ formulation," *COMPEL: The International Journal for Computation and Mathematics in Electrical and Electronic Engineering*, vol. 28, no. 4, pp. 1059–1067, 2009.

[56] ——, "Fixed-point method for solving non linear periodic eddy current problems with $\mathbf{T}$, $\Phi - \Phi$ formulation," *Magnetics, IEEE Transactions on*, vol. 45, no. 3, pp. 948–951, 2009.

[57] *ANSYS 11.0 documentation*, SAS IP Inc., Canonsberg., 2007.

[58] Perrin-Bit, R. and Coulomb, J.L., "A three dimensional finite element mesh connection for problems involving movement," *Magnetics, IEEE Transactions on*, vol. 31, no. 3, pp. 1920 –1923, may 1995.